AD NUMBER
AD814672
LIMITATION CHANGES

TO:

Approved for public release; distribution is unlimited.

FROM:

Distribution authorized to U.S. Gov't. agencies and their contractors; Administrative/Operational Use; 31 JAN 1967. Other requests shall be referred to Air Force Technical Applications Center, Washington, DC 20333.

AUTHORITY

AFTAC USAF ltr 25 Jan 1972

AD814672

DDC

RECEIVED

MAY 2 9 1967

B

SCIENCE SERVICES DIVISION

TEXAS INSTRUMENTS
INCORPORATED

DESIGN OF SIGNAL-EXTRACTION FILTERS
USING LOCAL SIGNAL AND NOISE

ARRAY RESEARCH
SPECIAL REPORT NO. 20

Prepared

by

Paul R. Lintz

Program Manager
George C. Burrell

TEXAS INSTRUMENTS INCORPORATED
P. O. Box 5621
Dallas, Texas 75222

Contract No. AF 33(657)-12747
ARPA Order No. 104-60
Project Code No. 8100

Prepared for

AIR FORCE TECHNICAL APPLICATIONS CENTER
VELA Seismological Center
Washington, D. C. 20333

31 January 1967

ABSTRACT

This report discusses the use of multichannel filters designed from local signal and local noise in order to overcome the problem of gain inequalization. Included in this study is an analysis of the filtered outputs of several teleseisms and quarry blasts in order to determine whether the signal rejection noted in a previously developed filter was due to gain inequalities. Also included is an investigation of the use of various array geometries in the design of multichannel filters.

From this study, it can be concluded that:

- Use of local signal and noise in the design of signal-extraction multichannel filters is an effective technique for overcoming gain inequalities while preserving signal and rejecting a reasonable amout of noise

- A comparison of the outputs of local noise filter MCF A1 and IP 9 indicates that IP 9 exhibits excessive gain attenuation for teleseismic signals, which could be caused by either gain inequalities in the noise model or by an insufficient amount of gain variation added to the signal model

- Variations in the design signal-to-noise (S/N) ratios produces no significant gain in S/N improvement

- Filters designed using different array geometries show only slight variations in their final output

TABLE OF CONTENTS

TABLE

LIST OF ILLUSTRATIONS

science services division

LIST OF ILLUSTRATIONS (CONTD)

SECTION I
INTRODUCTION

The main purpose of this study was to use multichannel filters designed from local signal and noise in order to overcome gain inequalization problems. Another purpose was to determine whether gain inequalities were present in a previously developed filter. A third purpose was to investigate the use of various array geometries for the design of MCF's.

Signal-extraction filters were designed using local noise and signals from four events (two teleseisms and two quarry blasts) taken from the 1963 CPO data library.[*] Figure 1 shows the three CPO array geometries used in the design of the multichannel filters: one 5-channel ring-summed geometry; one 4-ring 2-triplet geometry; and one 2-ring 4-triplet geometry. The signal model was composed of signal plus noise taken over the time gate of the event. Signal-to-noise ratios were adjusted by scaling up or down the signal model. In addition, IP 9[**] was applied to one of the events and compared to MCF A1, the local noise filter.

---

[*] Texas Instruments Incorporated, 1965: Array Research, Semiannual Tech. Rpt. No. 4, Sec. VIII, Contract AF 33(657)-12747, 15 Dec.

[**] Baldwin, Dick: Transient Response Improvement for CPO Multichannel Filter Systems, Pt. I, (unpublished report for TI internal distribution).
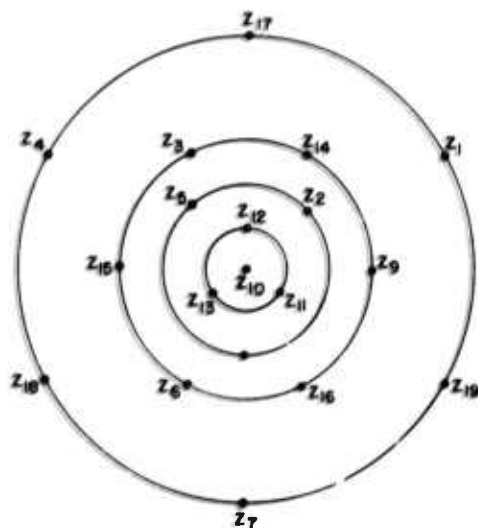
MCF A
19 SEISMOMETERS
5 RINGS
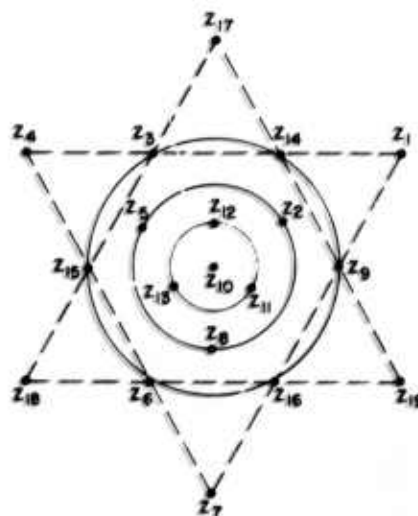
MCF B
19 SEISMOMETERS
4 RINGS
2 TRIPLETS
TRIPLET 1: $Z_1 + Z_4 + Z_7$
TRIPLET 2: $Z_{17} + Z_{18} + Z_{19}$
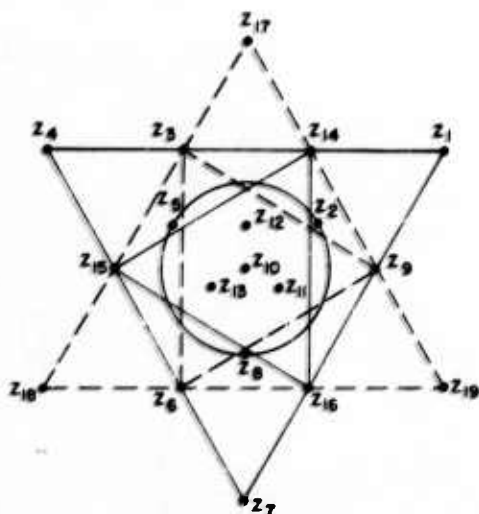
MCF C
16 SEISMOMETERS
2 RINGS
4 TRIPLETS
TRIPLET 1: $Z_1 + Z_4 + Z_7$
TRIPLET 2: $Z_{17} + Z_{18} + Z_{19}$
TRIPLET 3: $Z_{14} + Z_{15} + Z_{16}$
TRIPLET 4: $Z_3 + Z_6 + Z_9$

Figure 1. Array Geometries for CPO

SECTION II
GAIN INEQUALITIES

The "gain equalization" problem (resulting from different seismometers operating at different gains) is frequently encountered in the design of multichannel signal-extraction filters using a theoretical signal model and measured noise. This gain inequalization has two undesirable results. First, gain inequalities lead to signal distortion in the final summed output of the multichannel filter. Second, and even more serious, a filter designed on the basis of gain inequality could attempt to separate signal from noise on this basis rather than on the basis of velocity and $\vec{k}$-space separation.

A. DESIGN OF A PARTICULAR MCF ON THE BASIS OF GAIN INEQUALITY

To show how a multichannel filter could separate signal from noise on the basis of gain inequality, the following simple example is presented. This example, by John Burg,[*] is based upon a 2-channel array (Figure 2).

CHANNEL 1 $S_1(t) + N_1(t)$ ——→ $h_1(t)$

CHANNEL 2 $S_2(t) + N_2(t)$ ——→ $h_2(t)$

Σ ——→ P(t)
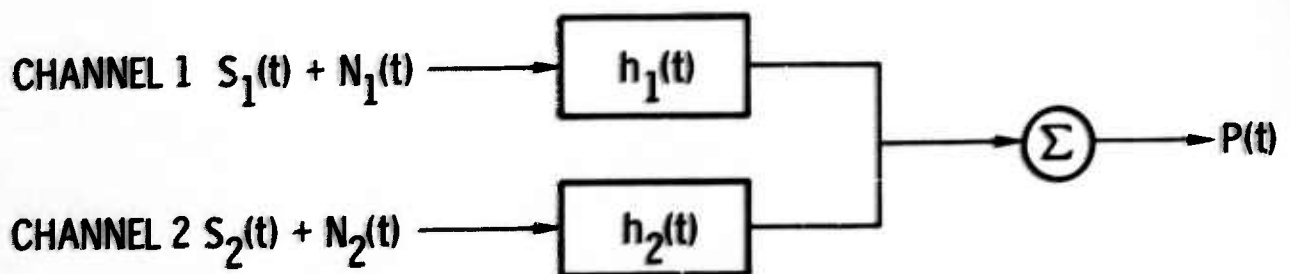
Figure 2. 2-Channel MCF

[*]Burg, John, 1966: Texas Instruments Seminar on Multichannel Filtering.

The problem is to design a 2-channel MCF using a theoretical signal model and measured noise. Assuming that the output of each of the two channels is identical, except that channel 2 is scaled by a factor of "a", the output of the multichannel filter using an equalized signal would be

$$P(t) = \left[S_1(t) + N_1(t) \right] * h_1(t) + \left[S_1(t) + a N_1(t) \right] * h_2(t)$$

where

$\quad\quad P(t) \quad$ is the output of the MCF

$\quad h_1(t), h_2(t) \quad$ are filters for channels 1 and 2, respectively

$\quad\quad t \quad$ is time

$\quad a \neq 1$

By using a 1-point multichannel filter, the situation could occur in which the filter rejects the unequalized measured noise and passes the entire equalized theoretical signal. This case occurs if $h_1(t)$ and $h_2(t)$ are chosen such that

$$h_1(t) = -a h_2(t)$$

and

$$h_1(t) = 1 - h_2(t)$$

or, in terms of a,

$$h_1(t) = \frac{1}{1 - \frac{1}{a}} = \frac{a}{a - 1}, \quad h_2(t) = -\frac{1}{a - 1}$$

4

Then the output of the MCF for a theoretical signal would be

$$P(t) = \left[S_1(t) + N_1(t)\right]\left(\frac{a}{a-1}\right) + \left[S_1(t) + a\,N_1(t)\right]\left(-\frac{1}{a-1}\right)$$

or

$$P(t) = \left\{\frac{a}{a-1} - \frac{1}{a-1}\right\} S_1(t) + \left\{\frac{a}{a-1} - \frac{a}{a-1}\right\} N_1(t) = S_1(t)$$

In this case, the MCF would pass the signal model perfectly and reject the noise perfectly. Hence, the mean-square-error would be zero, and the S/N improvement

$$\left(\frac{\dfrac{\text{signal out}}{\text{signal in}}}{\dfrac{\text{noise out}}{\text{noise in}}}\right)$$

would be infinite.

If this MCF were then used to process actual unequalized signal and noise, the output would be

$$P(t) = \left[S_1(t) + N_1(t)\right]\left(\frac{a}{a-1}\right) + \left[a\,S_1(t) + a\,N_1(t)\right]\left(\frac{1}{a-1}\right)$$

or

$$P(t) = 0$$

Hence, both signal and noise would be entirely rejected.

B. METHODS OF OVERCOMING GAIN INEQUALITY

In MCF design, gain inequality is important only in the low frequency region, since noise is highly coherent and approximately identical on each channel at low frequencies.

The following four factors, taken together, may indicate that an MCF has been designed on the basis of gain inequality:

- The output of the MCF will exhibit attenuation of signal

- The MCF will exhibit an unusually large amount of S/N improvement relative to the theoretical signal at low frequencies

- The f-$\vec{k}$ (3-dimensional Fourier transform) response of the filter will not show as much rejection of noise (in db) as the S/N improvement curve indicates

- The MCF will exhibit high gains on a few individual channels

While none of the preceding factors considered individually is sufficient proof that a filter has been designed on the basis of gain inequality, the presence of all factors would be quite conclusive. Also, the presence of the second and third factors alone generally shows that the filter has been designed on the basis of gain inequality.

A good indication of the amount of MCF signal attenuation is obtained by examining the "error trace" (the "noise rejection trace"). The error trace is formed by subtracting the output of the MCF from the output of the reference seismometer of the array. The time trace thus formed is an indication of what the MCF is rejecting as noise on the reference seismometer's output. If there is a noticeable change in the complexity of the error trace over the time gate for the signal, the MCF is rejecting part of the signal.

science services division

A comparison of the power density spectra of the error trace taken over the time gate preceding the signal with that taken over the time gate during the signal event gives a good estimate of the amount of signal power being rejected. However, if too short a time gate is taken, the noise power will not be statistically stable. Therefore, care should be taken in the analysis of such spectra. Nevertheless, the error or noise rejection trace is a useful tool in the analysis of multichannel filters.

There are several techniques available for overcoming gain inequalization:

- First, the original data could be equalized in amplitude or in both amplitude and phase. Amplitude equalization may be performed at a specific frequency or over a frequency band by first using a bandpass filter and then equalizing the trace amplitudes. Amplitude and phase equalization may be done using single-channel Wiener prediction filters with one trace as the reference or signal trace.

- A second method is to add statistical gain fluctuation[*] to the theoretical signal model. The random signal can be added by scaling the autocorrelations of the signal model by a constant greater than 1. The effect of the random signal is to force the MCF to reduce the mean-square-error on the basis of the $f\text{-}\vec{k}$ spectrum of the noise model rather than on the basis of gain inequality.

[*]Texas Instruments Incorporated, 1965: Array Research, Semiannual Tech. Rpt. No. 4, Sec. IV, AF 33(657)-12747, 15 Dec.

- A third method of correcting for gain in-
  equalization is to use the signal plus noise
  on the reference seismometer as the desired
  signal. The noise model would then be the
  noise on each channel preceding the signal,
  and the signal model would be the signal plus
  noise on each channel. In this manner, gain
  inequalities and random signal would be built
  into the signal model (since, in practice, the
  signal would not exhibit perfect coherence
  between channels). The third method might
  also be a good technique for passing all phases
  (P, S and L-R) of an event.

SECTION III
MCF DESIGN AND RESPONSES

A. FILTER DESIGN

For this study, three basic filters were designed using three array geometries for each of four events. An additional filter (MCF A2) was designed for the Crete event in which the S/N ratio was changed to 1/10.

Both MCF A1 and MCF A2 are local noise and signal filters; MCF A1 has an S/N ratio of 1, while MCF A2 has an S/N ratio of 1/10.

IP 9 was designed using an equalized theoretical signal model and a local noise model.[*] Random signal was not added to its design. It was designed to pass teleseismic signals having an apparent horizontal velocity greater than 12.8 km/sec. IP 9 was chosen for comparison to MCF A1 because their design parameters (S/N ratio, number of channels, etc.) were similar and because IP 9 exhibited excessive signal attenuation. It was suspected that this excessive signal attenuation was caused by gain inequalities.

B. NOISE REJECTION

The error or noise rejection trace is a useful tool in signal-extraction work because a careful analysis of its power spectra gives a quantitative measure of the amount of signal being rejected. If the time gate of the noise is long enough to insure that the noise field is essentially time-stationary, the power spectrum of the noise trace preceding the signal should approximately equal the power spectrum of the error trace taken over the signal gate. The difference between these two spectra should give a good estimate of the amount of signal as a function of frequency being rejected.

---

[*] Baldwin, Dick, Transient Response Improvement for CPO Multichannel Filter Systems, Pt. I, (unpublished report for TI internal distribution).

If the filter is doing a perfect job, both power spectra should exactly equal the power spectra of the original noise input trace.

Figure 3 presents the outputs of MCF A1, MCF A2, IP 9, and the straight sum for the Crete teleseism. As is evident from Figure 3, MCF A1, MCF A2 and IP 9 do a fairly good job of rejecting noise and passing signal. Also, MCF A2 seems to reject more noise than do either MCF A1 or MCF A2. However, IP 9 also seems to attenuate the signal by an excessive amount. Figure 3 shows that the straight-sum trace rejects the high-frequency noise well but is not able to reject the low-frequency noise.

Figures 4, 6, 8, and 10 present the power spectra of the traces in Figure 3 and indicate that IP 9, MCF A1, MCF A2, and (sum of all channels)/19 reject signal to some extent. These figures show that IP 9 rejects a about 6 db more signal and noise than does MCF A1. Also, the difference between the signal error and the noise error curves is slightly larger for IP 9 than for MCF A1. The difference between the signal error curves and the noise error curve for MCF A2 is larger than for MCF A1, as was expected.

The noise out (N_{out}) curve is the difference between the noise in (N_{in}) and the noise error (N_{error}) curves. It is the frequency spectrum of the output of the MCF taken over the noise gate preceding the signal arrival. The difference between the N_{in} and N_{out} curves for each filter in Figures 5, 7, 9, and 11 indicates the amount of noise considered as signal by both the MCF's and the straight sum.

Figures 4 through 11 indicate that MCF A1 is doing a better job of preserving signal while rejecting noise than are any of the other filters. As expected, these figures show that changing the input S/N ratio results in either rejecting more signal in order to reject more noise or in passing more noise in order to pass more signal.
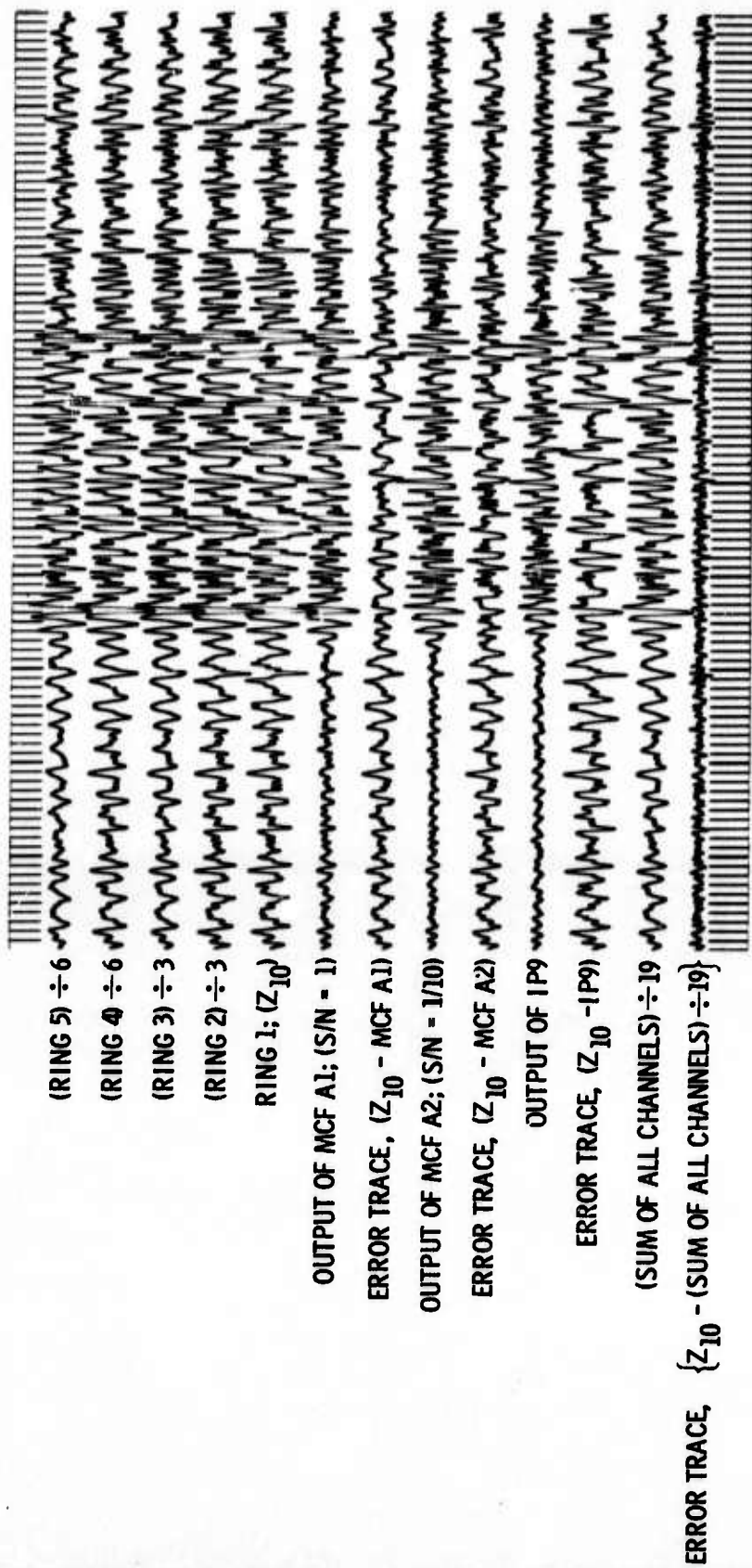
(RING 5) ÷ 6

(RING 4) ÷ 6

(RING 3) ÷ 3

(RING 2) ÷ 3

RING 1; (Z_{10})

OUTPUT OF MCF A1; (S/N = 1)

ERROR TRACE, (Z_{10} - MCF A1)

OUTPUT OF MCF A2; (S/N = 1/10)

ERROR TRACE, (Z_{10} - MCF A2)

OUTPUT OF IP9

ERROR TRACE, (Z_{10} - IP9)

(SUM OF ALL CHANNELS) ÷ 19

ERROR TRACE, {Z_{10} - (SUM OF ALL CHANNELS) ÷ 19}

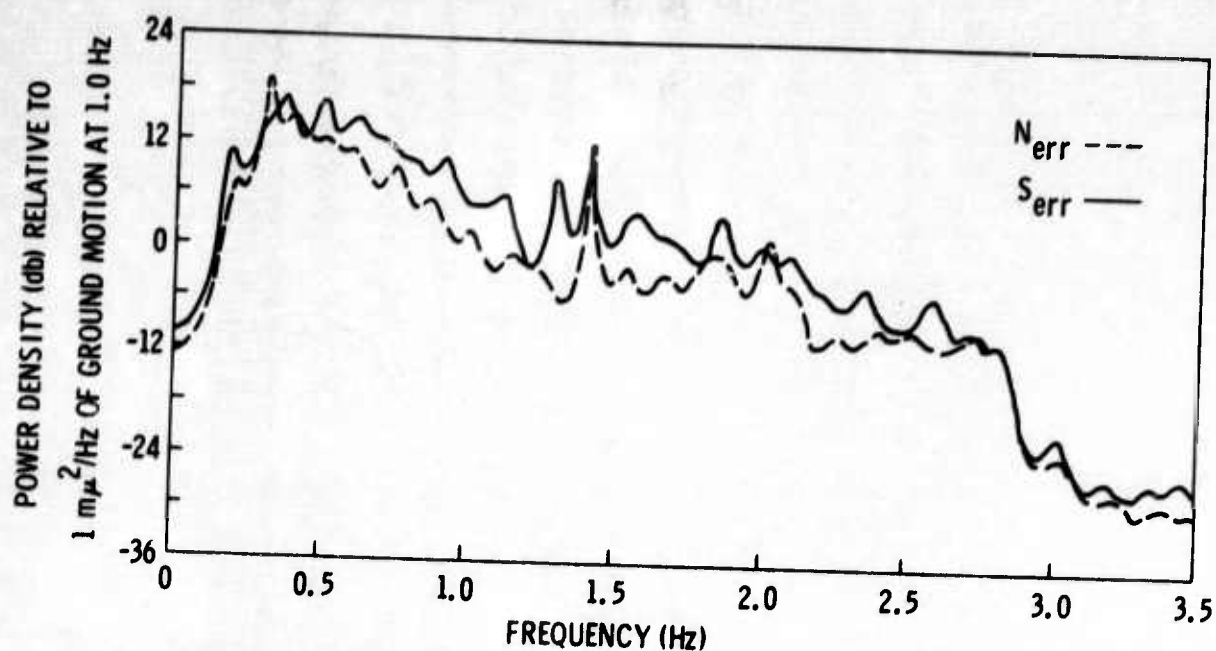Figure 3. Crete Teleseism ($\Delta = 85°$, $V = 22.5$ km/sec, $\theta = 50.14°$) with MCF and Straight-Sum Processing

science services division

Figure 4. Power Spectra for IP 9 Showing Signal Error and Noise Error
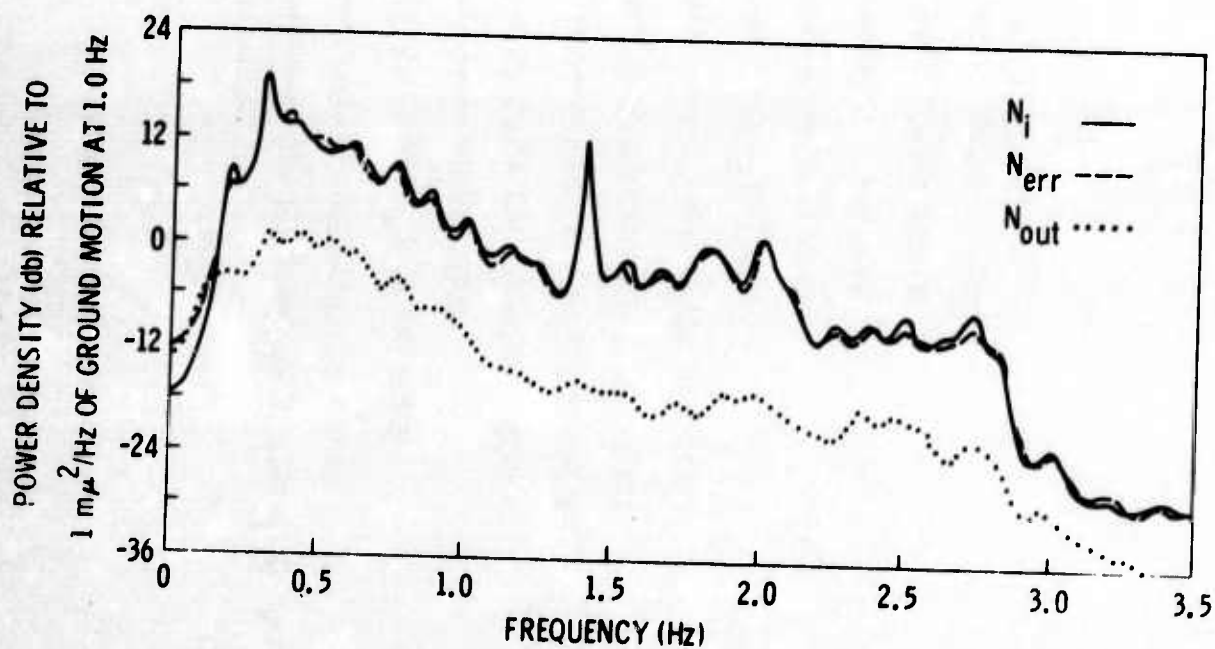
Figure 5. Power Spectra for IP 9 Showing Noise Error, Noise In and Noise Out
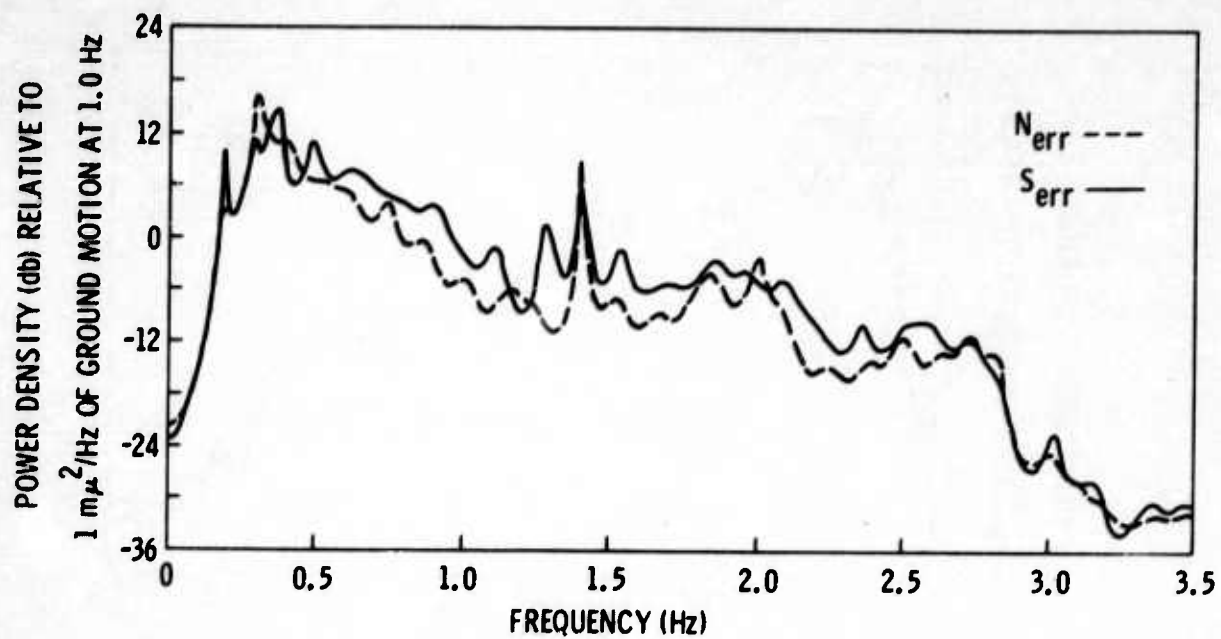
science services division

Figure 6. Power Spectra for MCF A1, S/N = 1, Showing
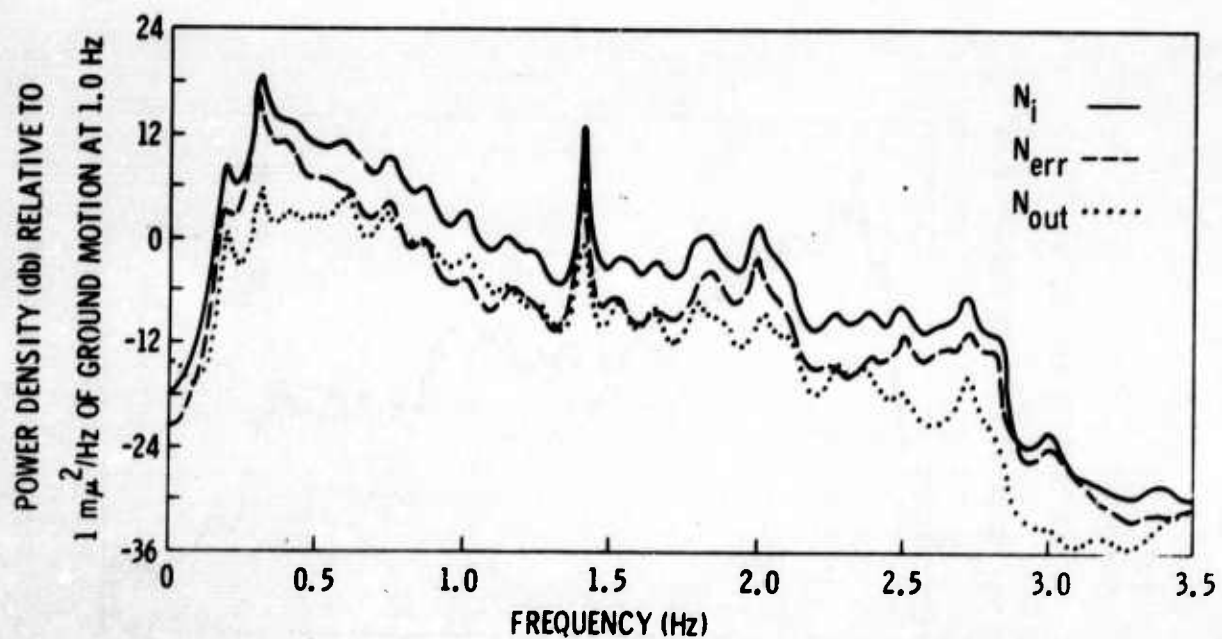Signal Error and Noise Error

Figure 7. Power Spectra for MCF A1, S/N = 1, Showing Noise
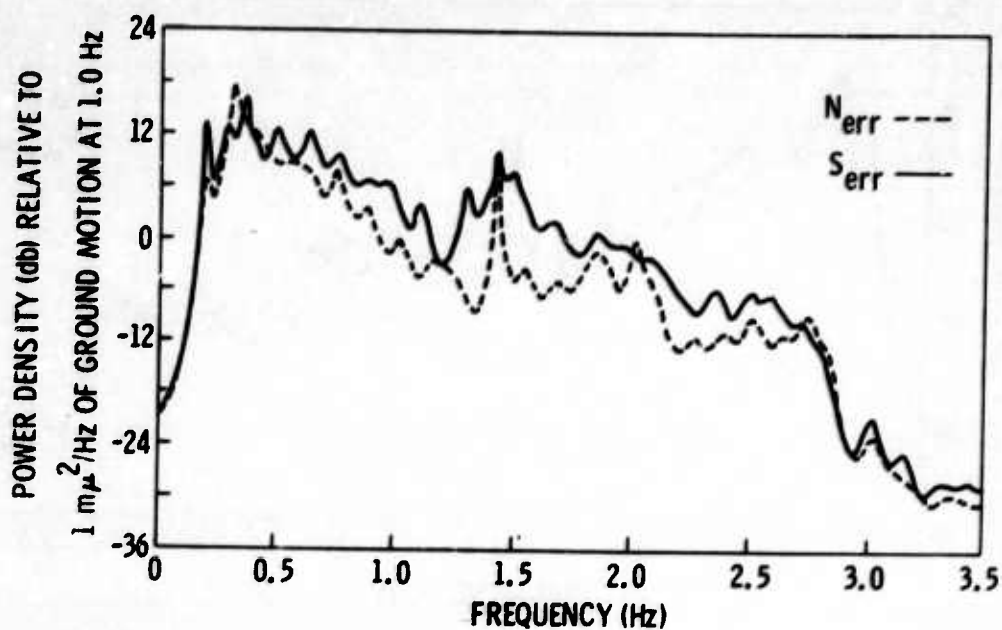Error, Noise In and Noise Out

13

Figure 8.   Power Spectra for MCF A2, S/N = 1, Showing
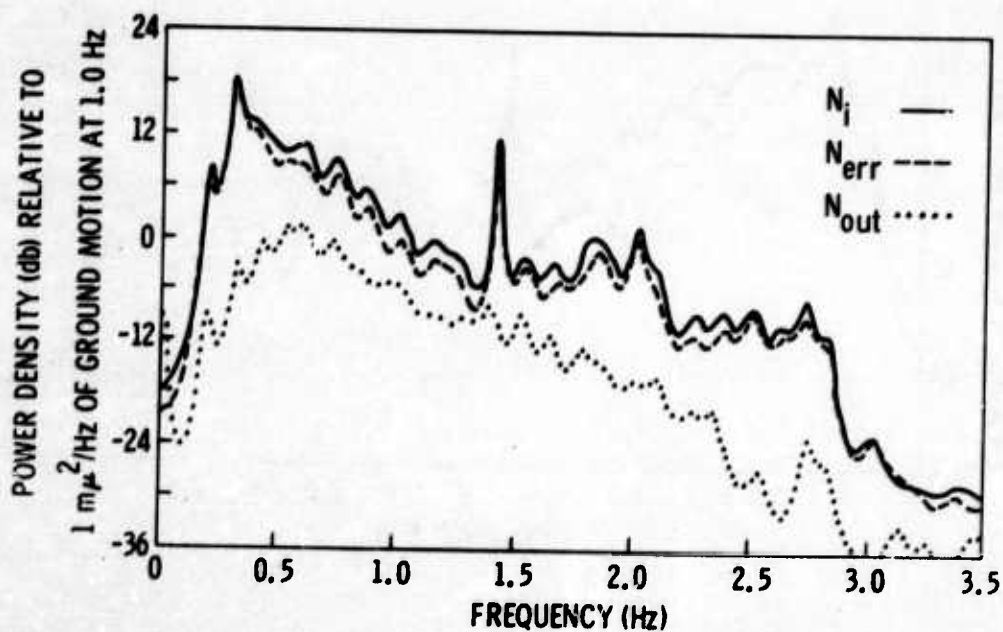Signal Error and Noise Error

Figure 9.   Power Spectra for MCF A2, S/N = 1, Showing
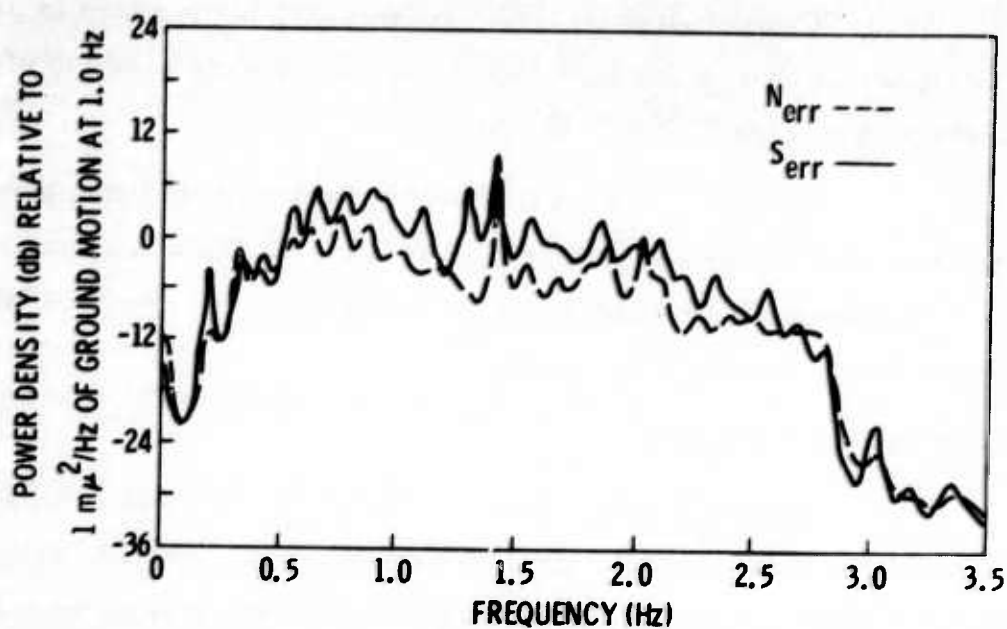Noise Error, Noise In and Noise Out

14

Figure 10. Power Spectra for (Straight Summation)/19
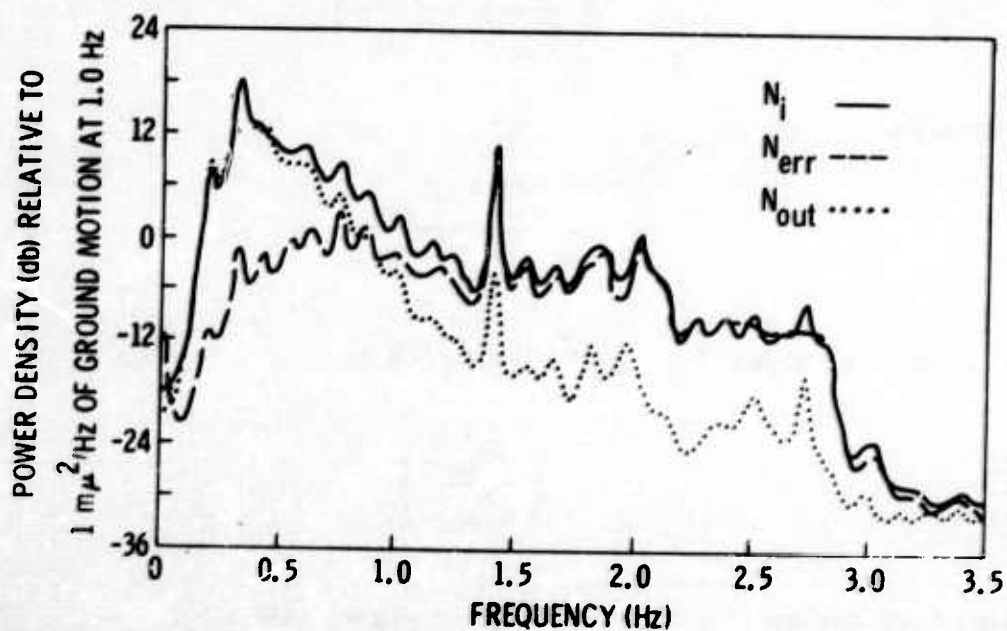Showing Signal Error and Noise Error

Figure 11. Power Spectra for (Straight Summation)/19
Showing Noise Error, Noise In and Noise Out

15   **science services division**

Figures 10 and 11 indicate that the straight sum is passing low-frequency noise (below 1.25 Hz) but is doing a very good job of rejecting high-frequency noise (above 1.25 Hz).

Figure 12 is the calculated response of IP 9 to a plane wave having the velocity and azimuth of the Crete event. This response was computed to determine if IP 9 should be rejecting the Crete event. It should not attenuate the amplitude of the signal.

C. S/N IMPROVEMENT

The $(N_{in}) \div (N_{out})$ curves, S/N improvement curves for the filters and the (sum of all channels)/19 are given in Figure 5, 13, 14, 15 and 16. The $(N_{in}) \div (N_{out})$ curves should be almost equal to the S/N improvement for an infinite velocity signal (as is the case for IP 9) if the response of the MCF is flat and equal to unity (0 db).

In Figures 13 through 16, S/N improvement

$$\left(\frac{S_{out}}{S_{in}}\right) \left(\frac{N_{in}}{N_{out}}\right)$$

is actually

$$\frac{(S + N)_{out}}{(S + N)_{in}}$$

taken over the signal time gate, multiplied by

$$\left(\frac{N_{in}}{N_{out}}\right)$$

taken over the noise gate preceding the signal gate.

Hence,

$$\left(\frac{S}{N} \text{ imp}\right)' = \left(\frac{S_{out} + N_{out}}{S_{in} + N_{in}}\right) \cdot \left(\frac{N_{in}}{N_{out}}\right)$$

$$= \left(\frac{S_{out} \, N_{in}}{S_{in} \, N_{out}}\right) \left(\frac{1 + \dfrac{N_{out}}{S_{out}}}{1 + \dfrac{N_{in}}{S_{in}}}\right)$$

$$= \left(\frac{S}{N} \text{ imp}\right) \cdot \left(\frac{1 + \dfrac{N_{out}}{S_{out}}}{1 + \dfrac{N_{in}}{S_{in}}}\right)$$

where

$\left(\dfrac{S}{N} \text{ imp}\right)$ is defined to be the true S/N improvement

$\left(\dfrac{S}{N} \text{ imp}\right)'$ is the calculated approximation of S/N improvement

These calculation are valid if the noise is time-stationary.

In regions where the average power of the signal input equals the average power of the noise input (if noise output << signal output),

$$\left(\frac{S}{N} \text{ imp}\right)' \simeq \frac{1}{2} \left(\frac{S}{N} \text{ imp}\right)$$

Thus, it is expected that $\left(\dfrac{S}{N} \text{ imp}\right)'$ would be approximately 6 db lower than the $(N_{in})/(N_{out})$ curves. This is approximately true below 0.75 Hz and above 2.0 Hz for Figures 13, 14 and 15.
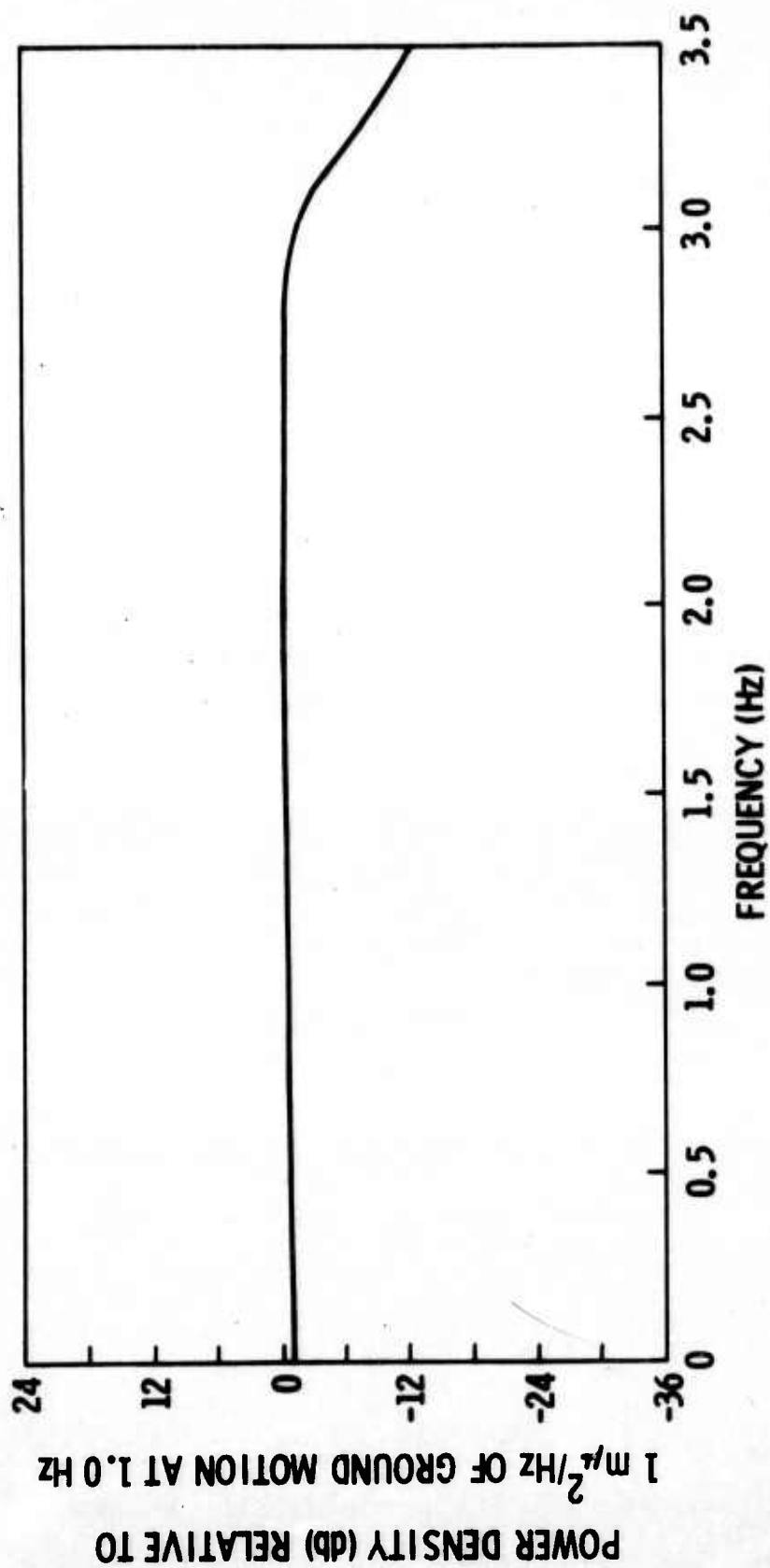
science services division

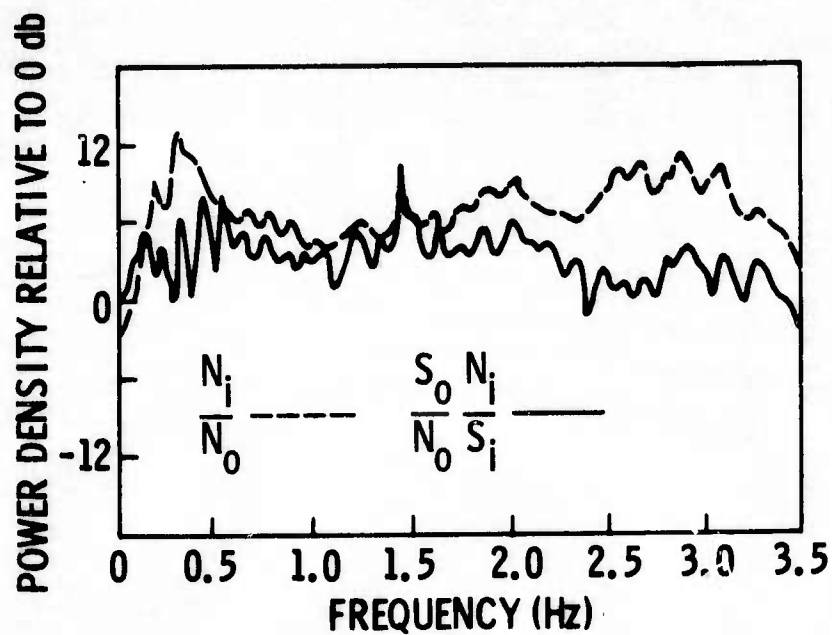Figure 12. Calculated IP 9 Response to a Plane Wave ($\theta = 50.14°$, $V = 22.5$ km)

Figure 13. (Noise In)/(Noise Out) and Signal-to-Noise
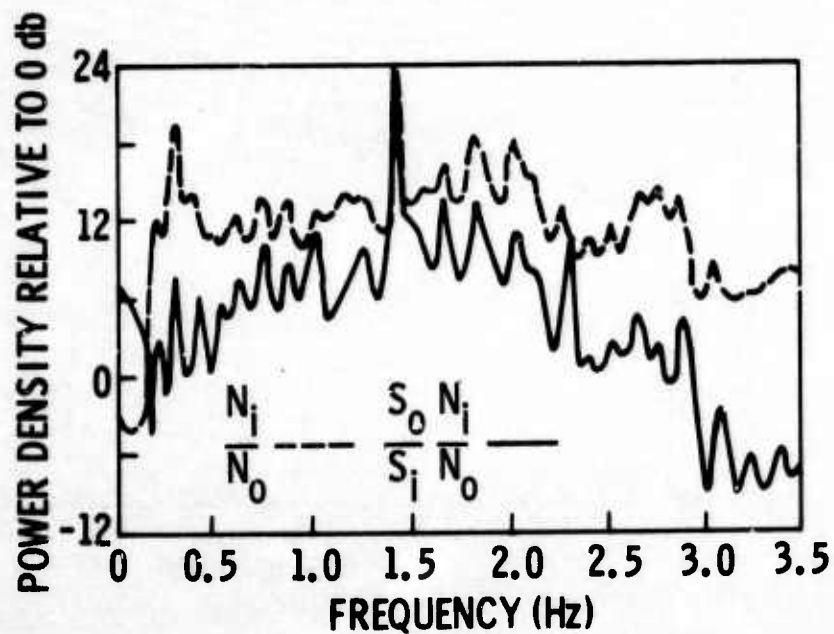Improvement Curves for MCF A1, S/N = 1

Figure 14. (Noise In)/(Noise Out) and Signal-to-Noise
Improvement Curves for IP 9
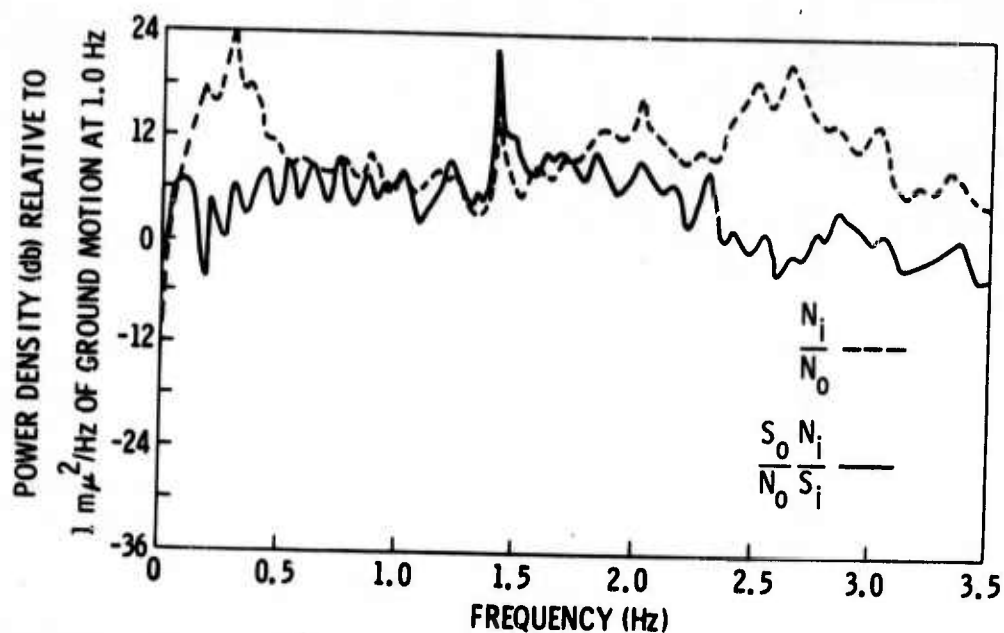
science services division

Figure 15.   (Noise In)/(Noise Out) and Signal-to-Noise
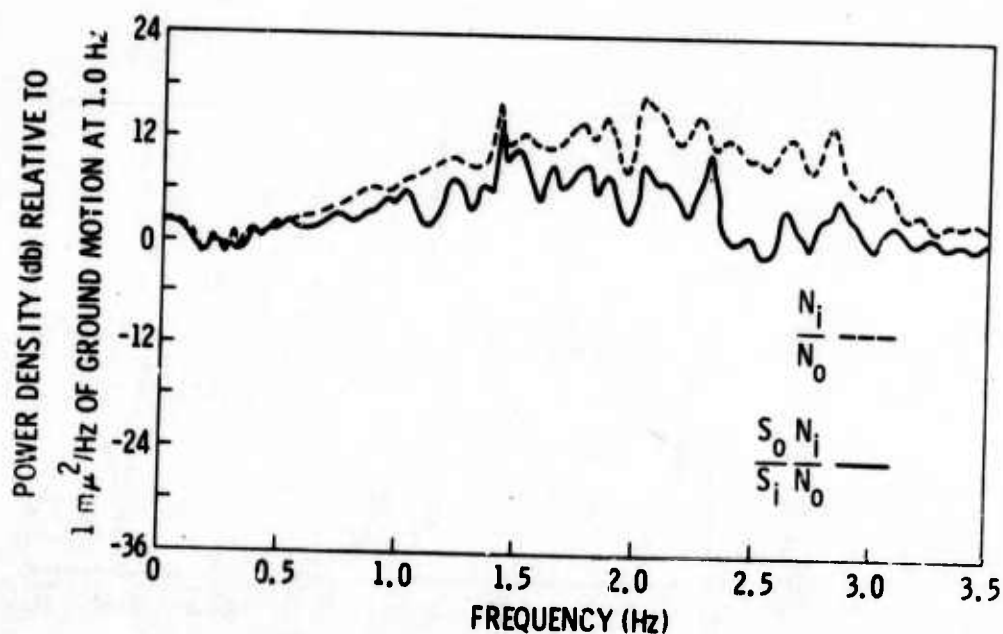Improvement Curves for MCF A2, S/N = 1/10

Figure 16.   (Noise In)/(Noise Out) and Signal-to-Noise Improvement Curves for (Straight Summation)/19

D. FREQUENCY-WAVENUMBER RESPONSES

Figures 17, 19, 21, 23, 25, 27, 29, 31, and 33 are f-$\vec{k}$ responses of MCF A1 at 0.1, 0.2, 0.25, 0.3, 0.4, 0.5, 0.75, 1.0 and 2.0 Hz, respectively. Figures 18, 20, 22, 24, 26, 28, 30, 32 and 34 are f-$\vec{k}$ responses of IP 9 at these same frequencies. (See pages 24 through 41.)

As mentioned previously, IP 9 shows excessive signal attenuation. However, S/N improvement curves relative to an infinite velocity model show that IP 9 does a fairly good job of noise and signal separation. Therefore, it is suspected that IP 9 separates signal from noise on the basis of gain inequality. The f-$\vec{k}$ responses for IP 9 should demonstrate whether the filter is doing as good a job as is shown by the S/N improvement curves. The f-$\vec{k}$ responses for MCF A1 were generated for some basis of comparison of the responses for IP 9.

As shown in Figures 17 and 18, both IP 9 and MCF A1 appear to be doing some velocity filtering, with MCF A1 rejecting somewhat higher velocity noise than does IP 9. MCF A1 also seems to be doing some frequency filtering since its power level is 6 db below that of IP 9 at 0.2 Hz. Both filters also are shown to separate signal from noise on the basis of velocity. However, IP 9 does not show signs of separating signal from noise (0.2 to 0.3 Hz) on the basis of gain inequality.

By studying the frequency-wavenumber responses, the following conclusions are reached:

- At 0.25 Hz, MCF A1 rejects a higher velocity noise than does IP 9. MCF A1 is clearly superior because its filter response begins dropping in $\vec{k}$-space at about 10 km/sec (rejecting energy with a velocity of less than 10 km/ ec), while the filter response of IP 9 does not begin dropping until approximately 4 km/sec.

- At 0.3 Hz, the response of MCF A1 begins dropping rapidly at about 6 to 7 km/sec, while IP 9 begins dropping rapidly at about 5 km/sec; however; the differences between the two responses are less than at 0.2 Hz.

- At 0.4 Hz, it would be difficult to choose one response as better than the other because of their similarity.

- At 0.5 Hz, MCF A1 begins dropping at approximately 14 to 15 km/sec, while IP 9 begins dropping at about 6 km/sec; otherwise, there is not much difference between the two.

- At 0.75 Hz, IP 9 rejects more low-velocity energy than does MCF A1 and, consequently, can perform more velocity separation.

- At 1.0 Hz, IP 9 again seems to do a much better job on the basis of velocity separation.

- At 2.0 Hz, IP 9 seems to reject more low-velocity energy than does MCF A1, but the difference between the two responses is not as great as at 0.75 and 1.0 Hz.

If the f-$\vec{k}$ responses are compared with the input noise spectrum (shown in Figure 5), several conclusions may be drawn. The N_{in} power spectrum indicates large peaks at 0.2, 0.3, 1.4, 1.8, and 2.0 Hz, with MCF A1 doing a good job of filtering at the peaks of coherence noise power. At frequencies above 2.0 Hz, IP 9 seems to do a much better job than does MCF A1; however, the noise appears random to a small array at these higher frequencies; therefore, no velocity separation can be expected. It is obvious from the f-$\vec{k}$ responses that IP 9 does not attempt to

separate signal from noise on the basis of gain inequality. Therefore, the
excessive attenuation of signal exhibited by IP 9 probably is due to the fact
that not enough gain variation has been added to the signal model. An
inspection of Figure 3 indicates that gain inequalities exist in the data due
to the summation of the data into rings. If these gain inequalities were to
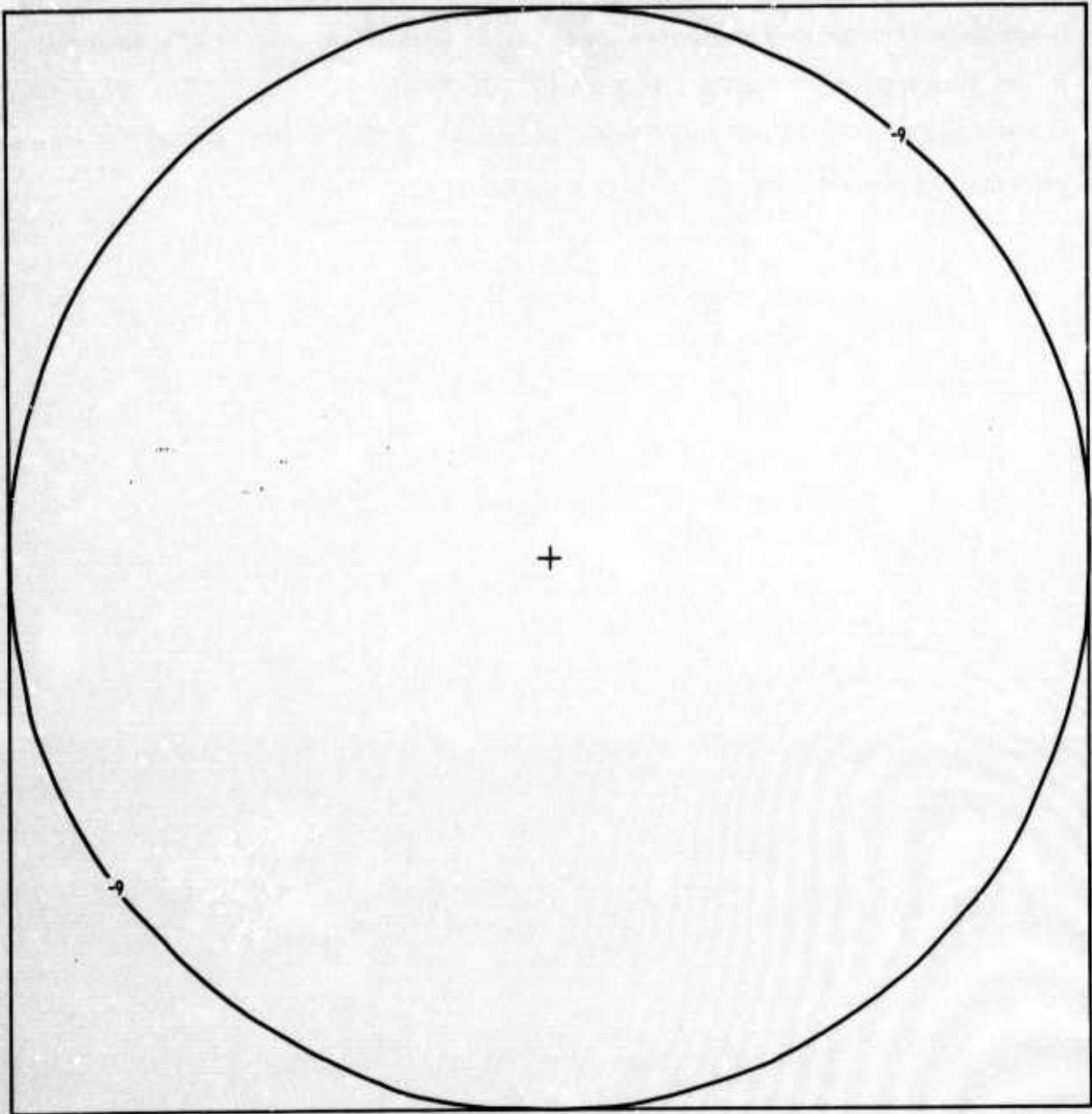exceed the amount of gain variation added to the IP 9 signal model, it would
be possible for IP 9 to attenuate the signal.

Figure 17.   MCF A1 f-$\vec{k}$ Response at 0.1 Hz

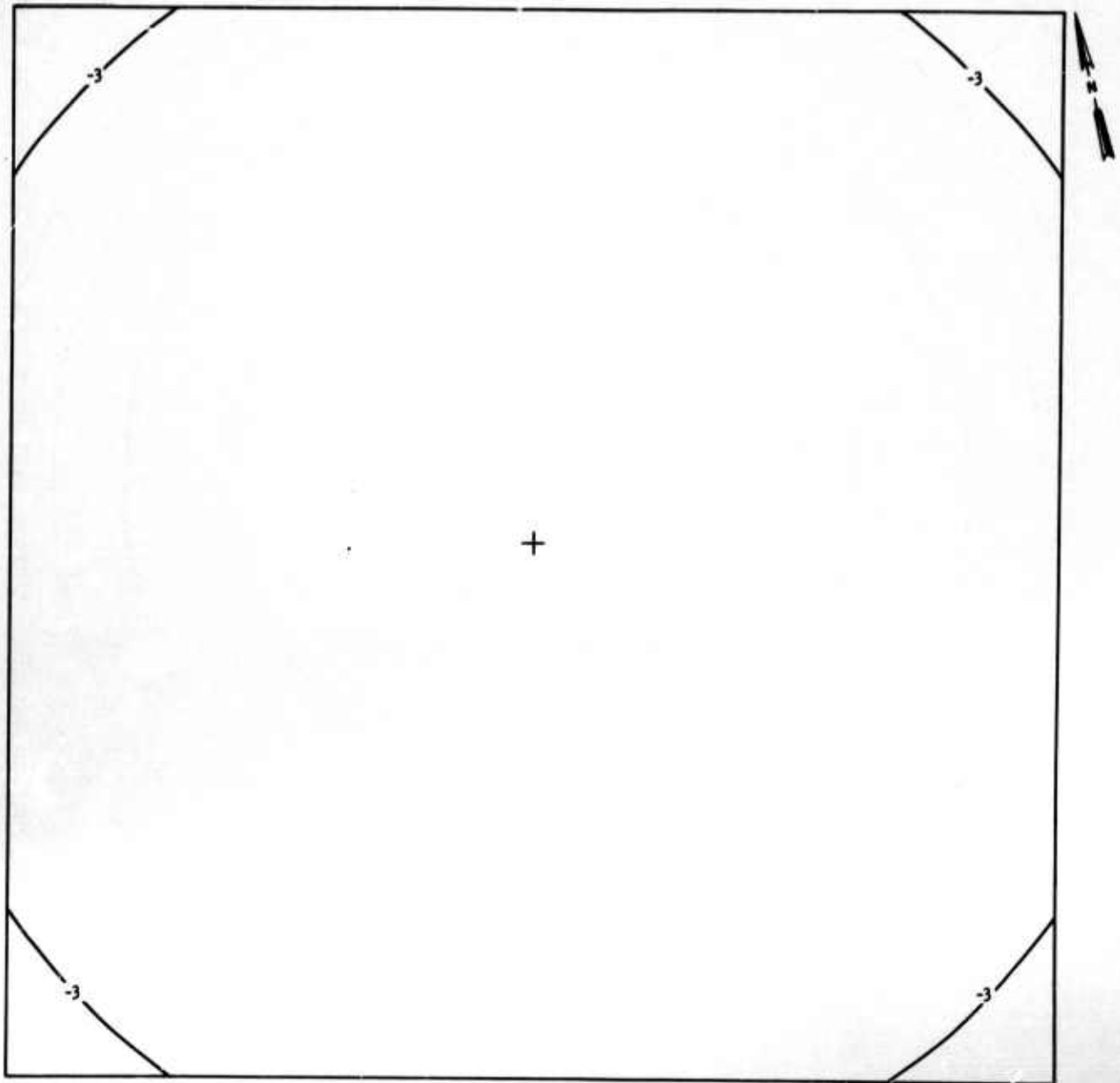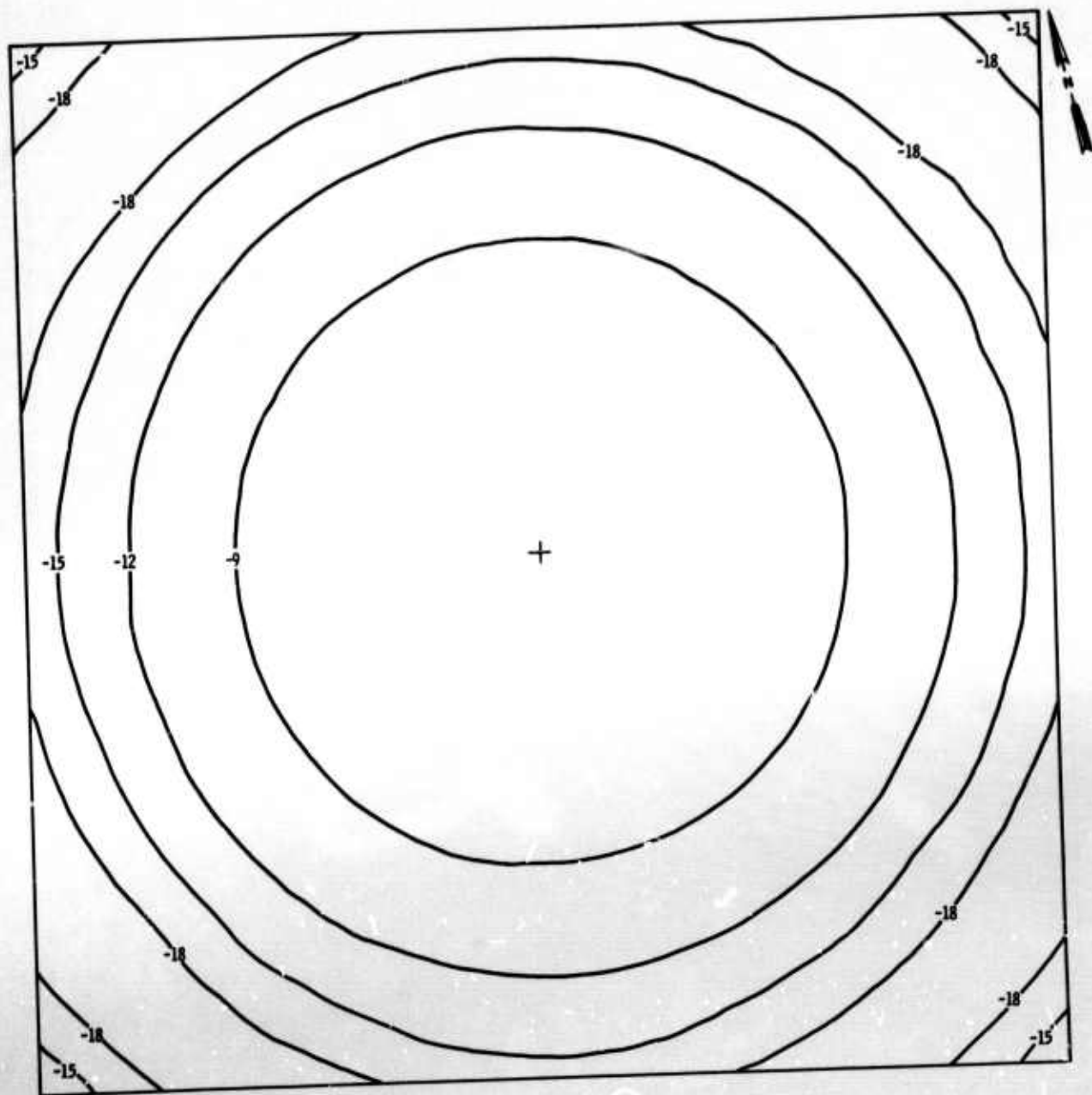Figure 18. IP 9 f-$\vec{k}$ Response at 0.1 Hz
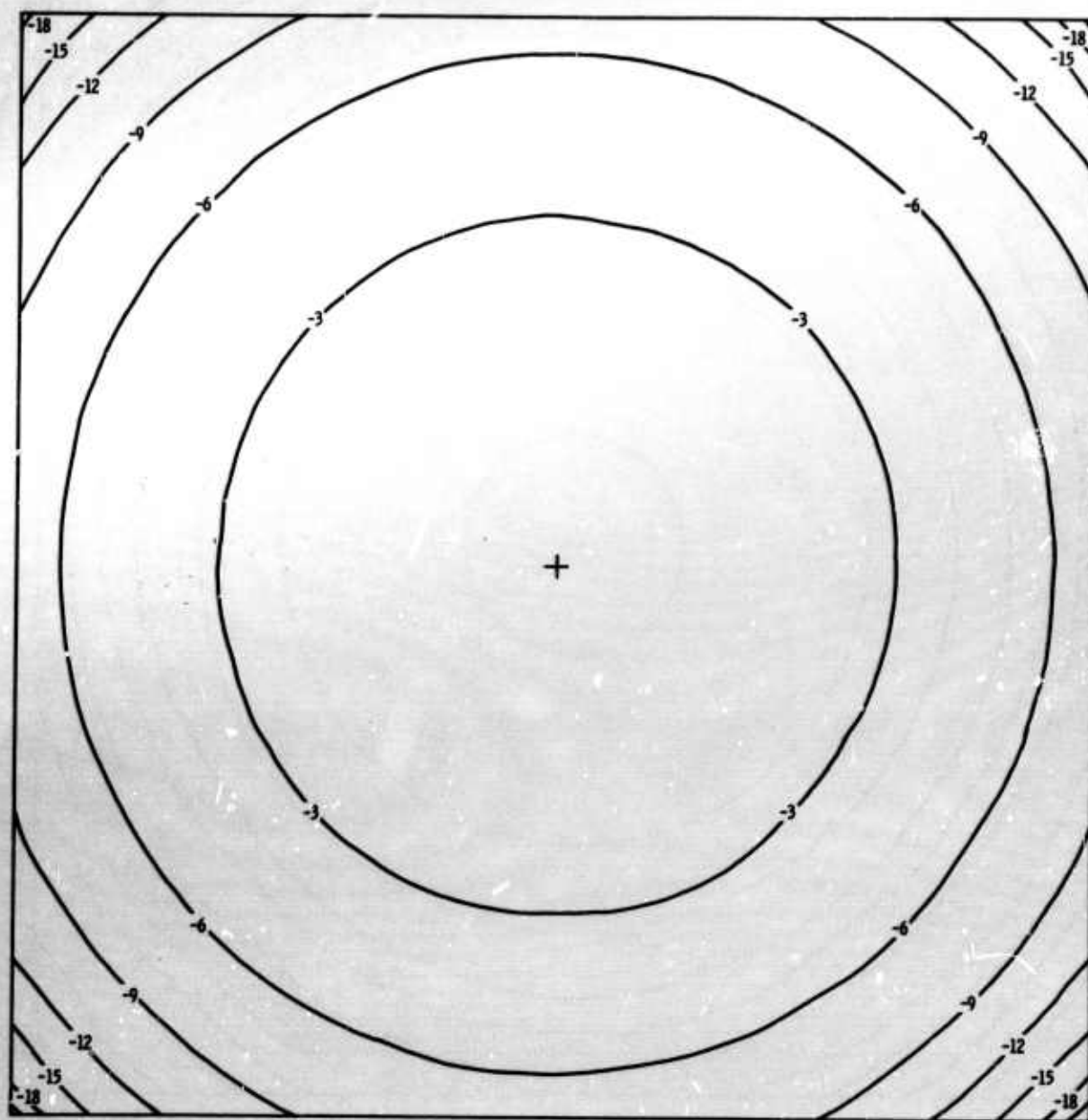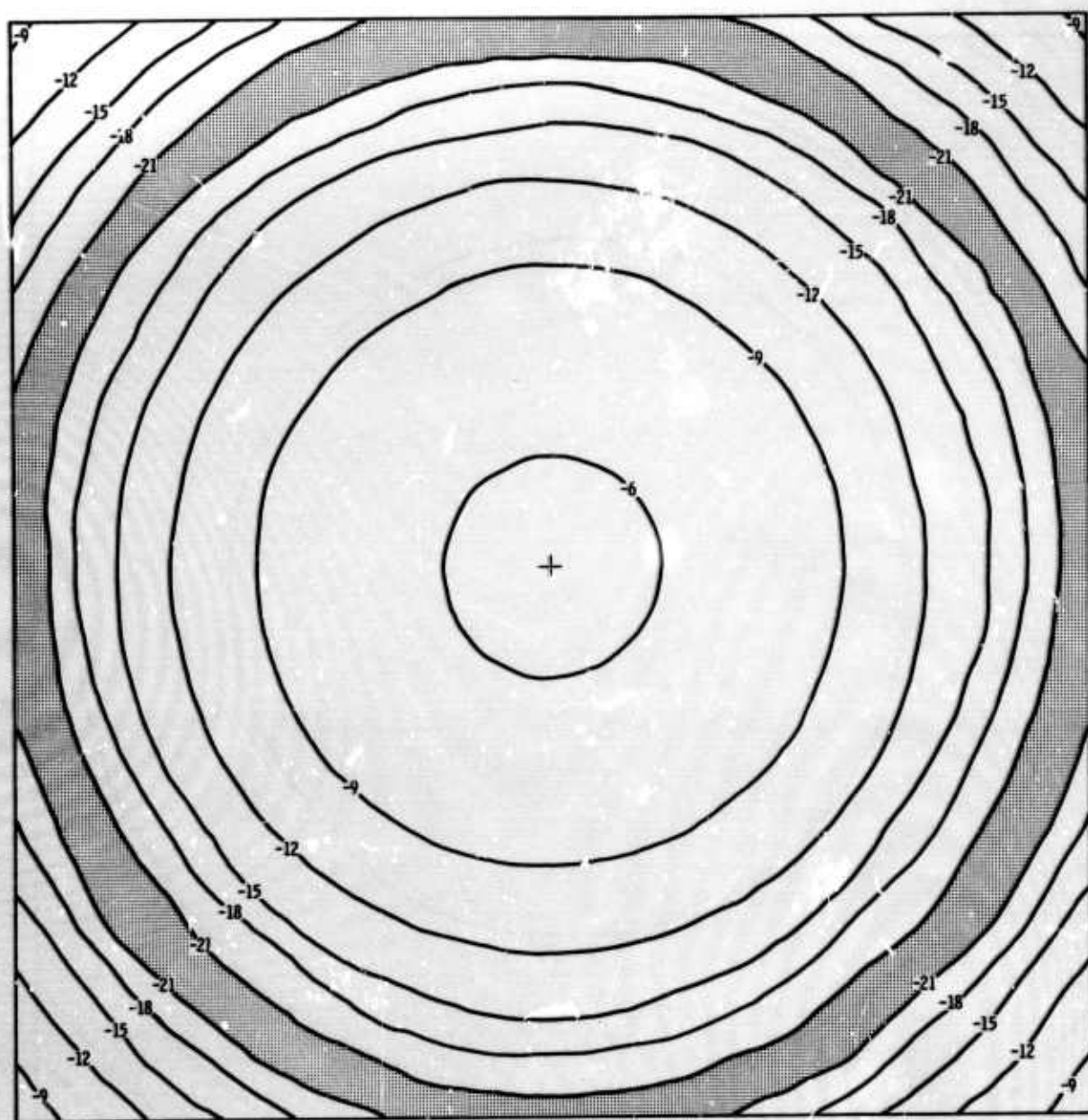
Figure 19. MCF Al f-$\vec{k}$ Response at 0.2 Hz

science services division

Figure 20. IP 9 f-$\vec{k}$ Response at 0.2 Hz

BELOW -21 db

Figure 21. MCF A1 f-k Response at 0.25 Hz, S/N = 1

science services division
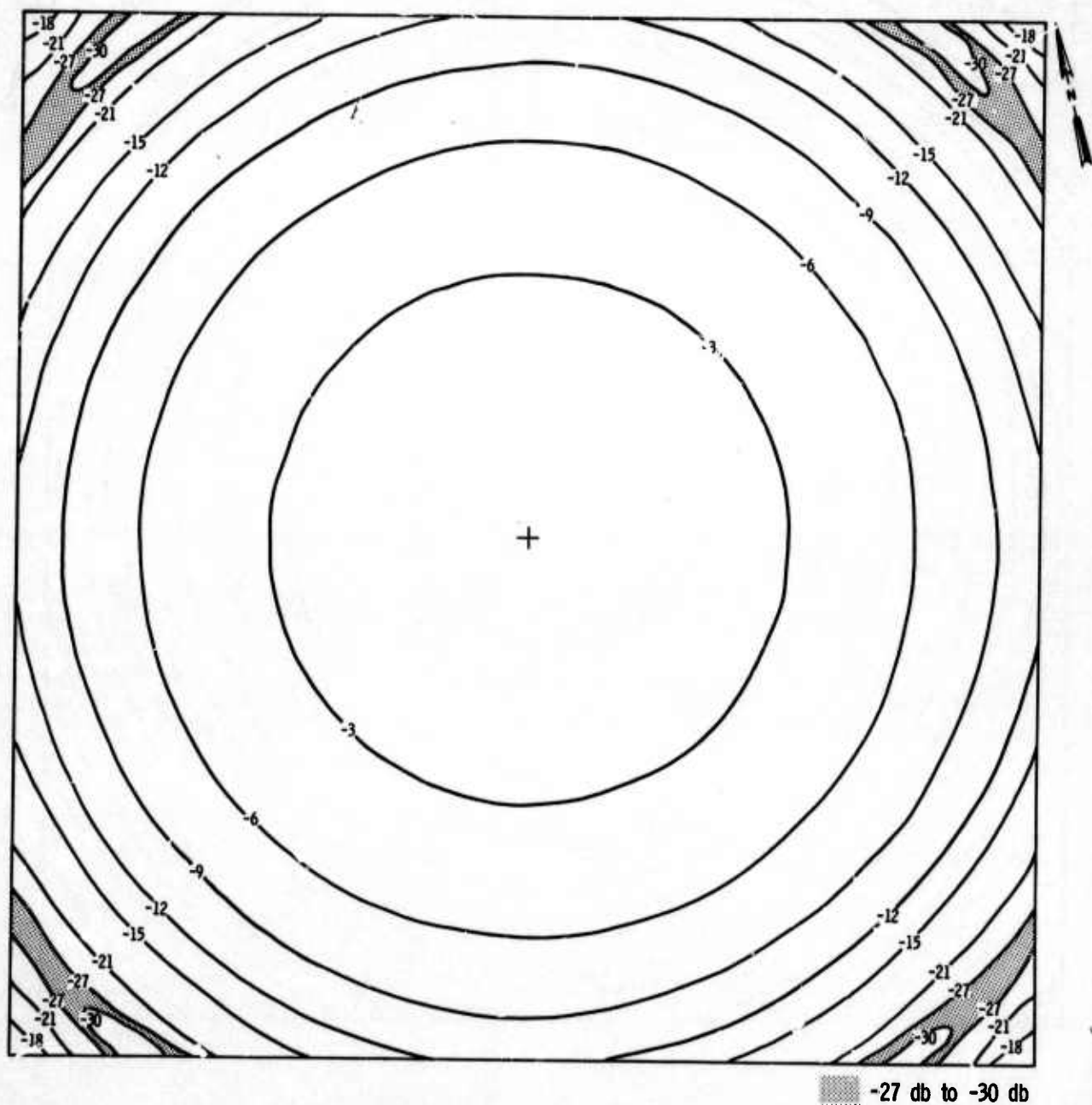
-27 db to -30 db

Figure 22. IP 9 f-$\vec{k}$ Response at 0.25 Hz
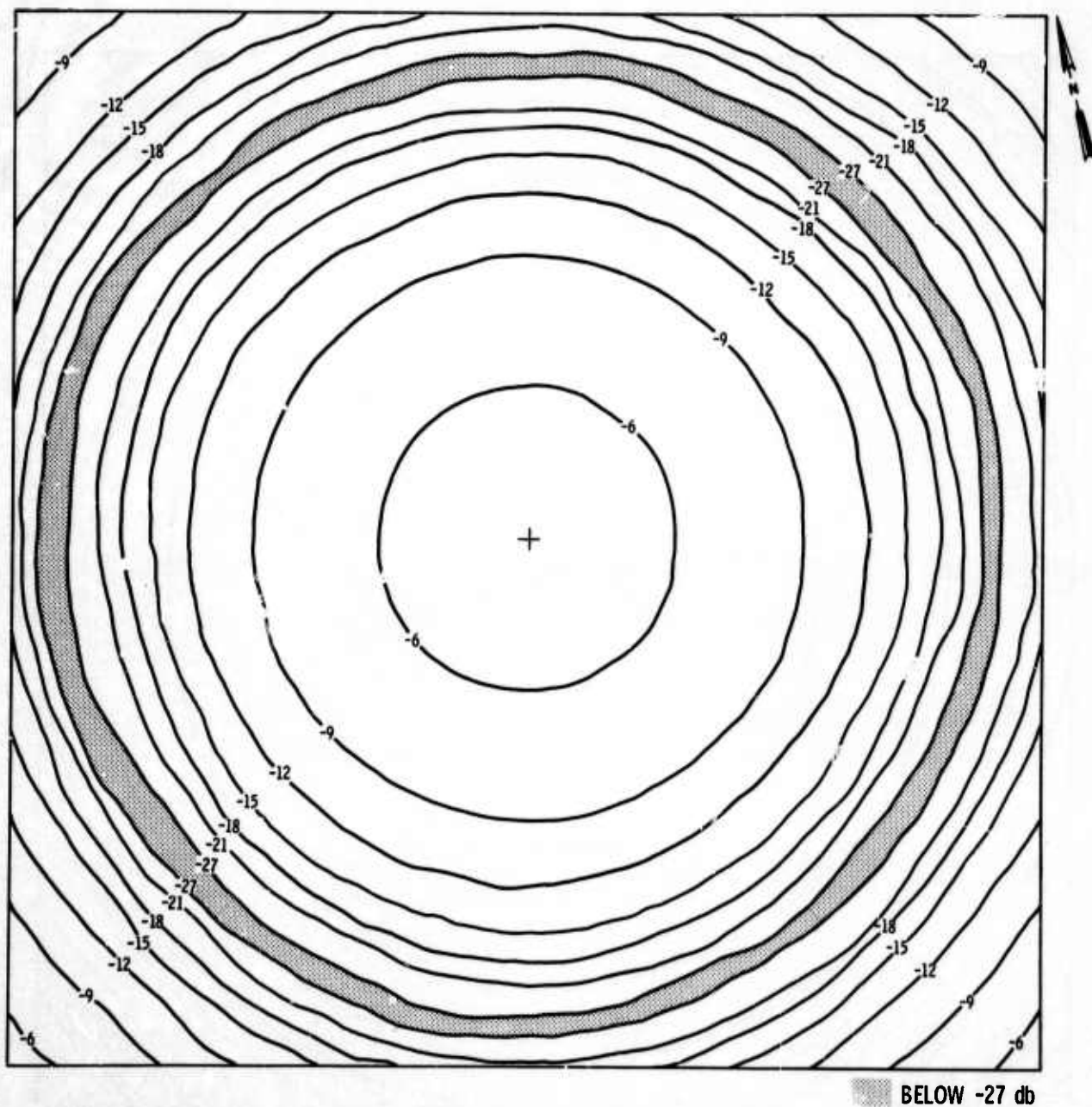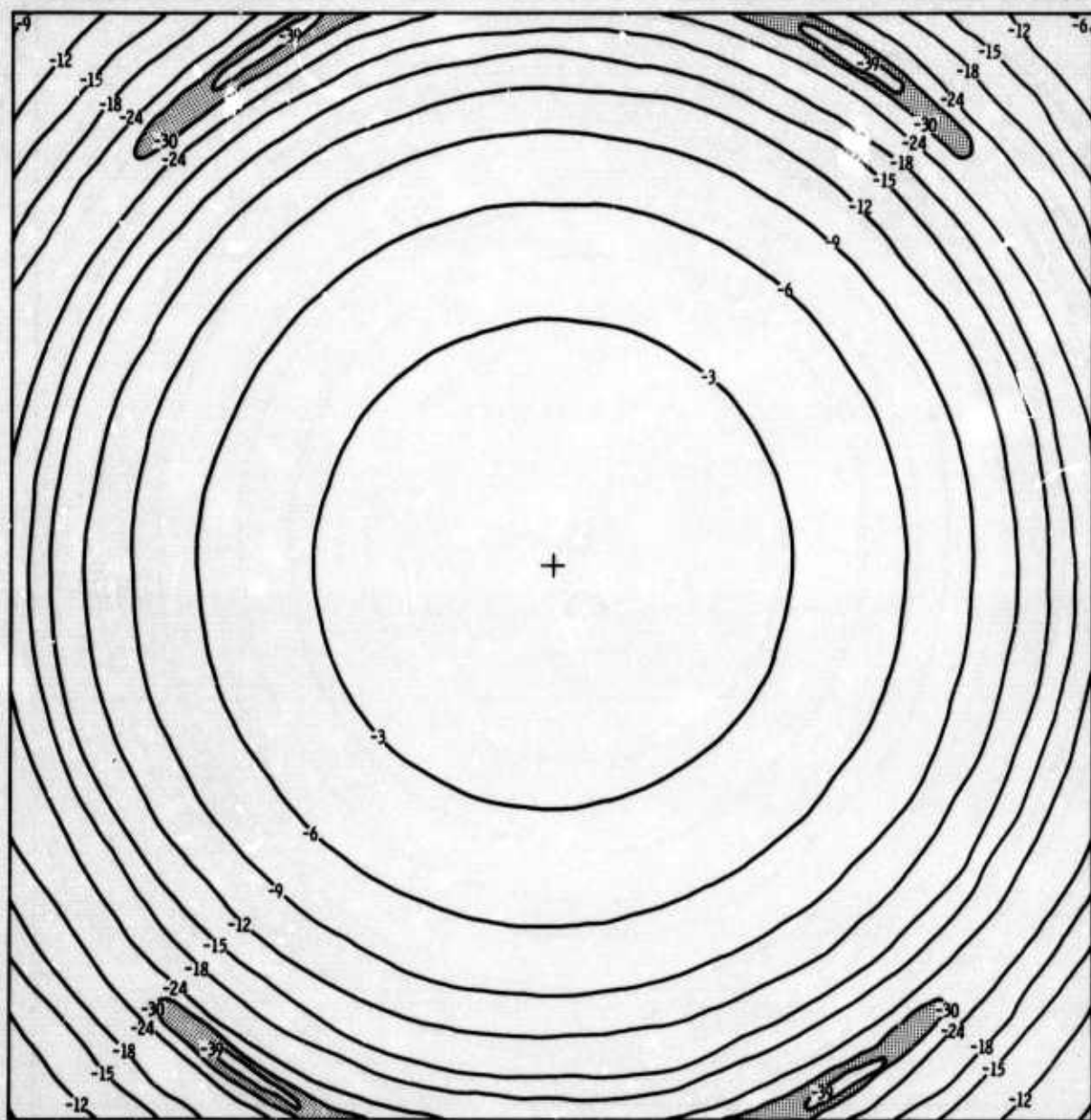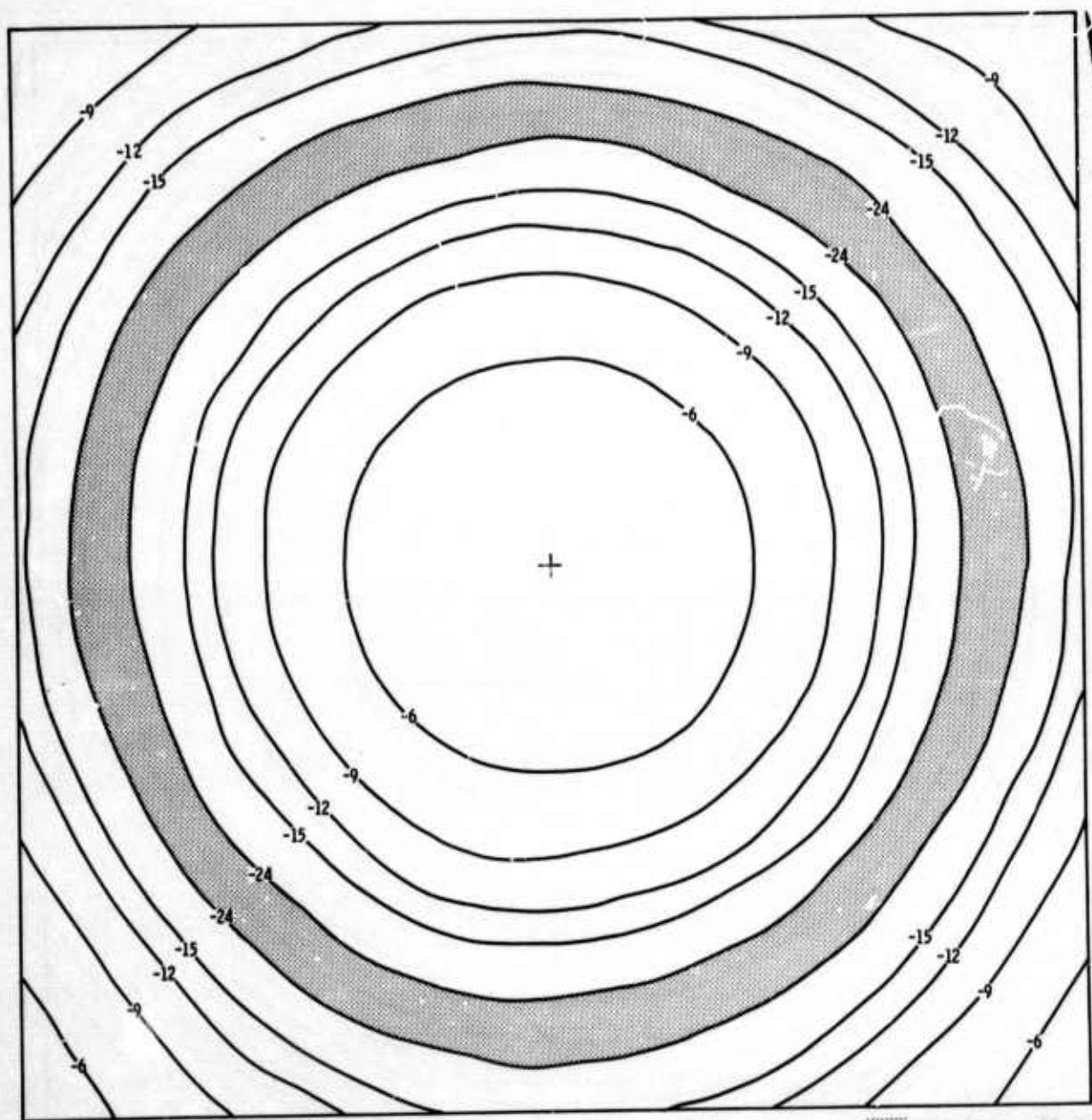
Figure 23. MCF A1 f-$\vec{k}$ Response at 0.3 Hz, S/N = 1

Figure 24. IP 9 f-$\vec{k}$ Response at 0.3 Hz

-30 db to -39 db

Figure 25. MCF A1 f-$\vec{k}$ Response at 0.4 Hz, S/N = 1

-24 db to - 36 db

science services division
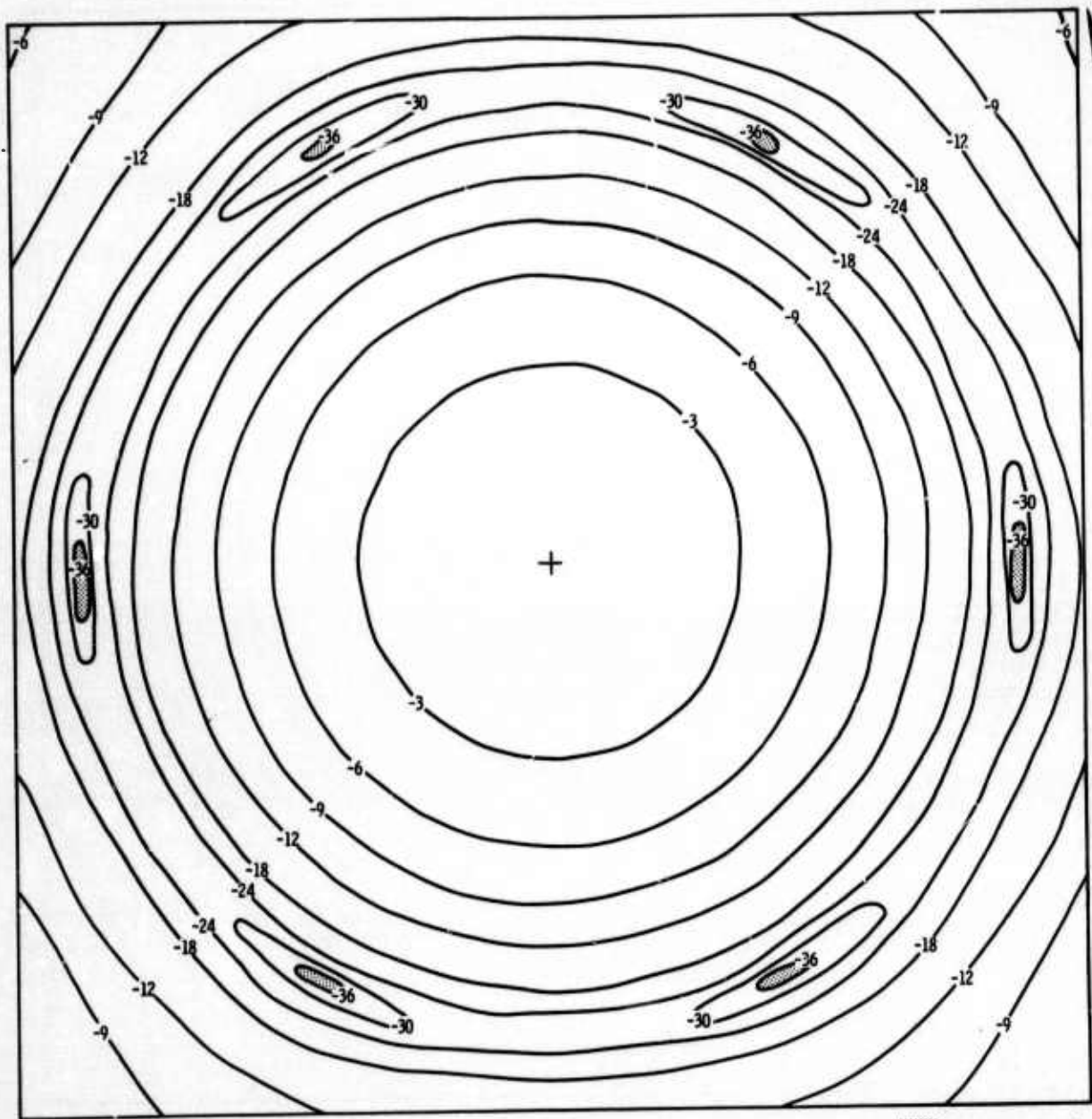
BELOW −36 db

Figure 26.   IP 9 f-$\vec{k}$ Response at 0.4 Hz

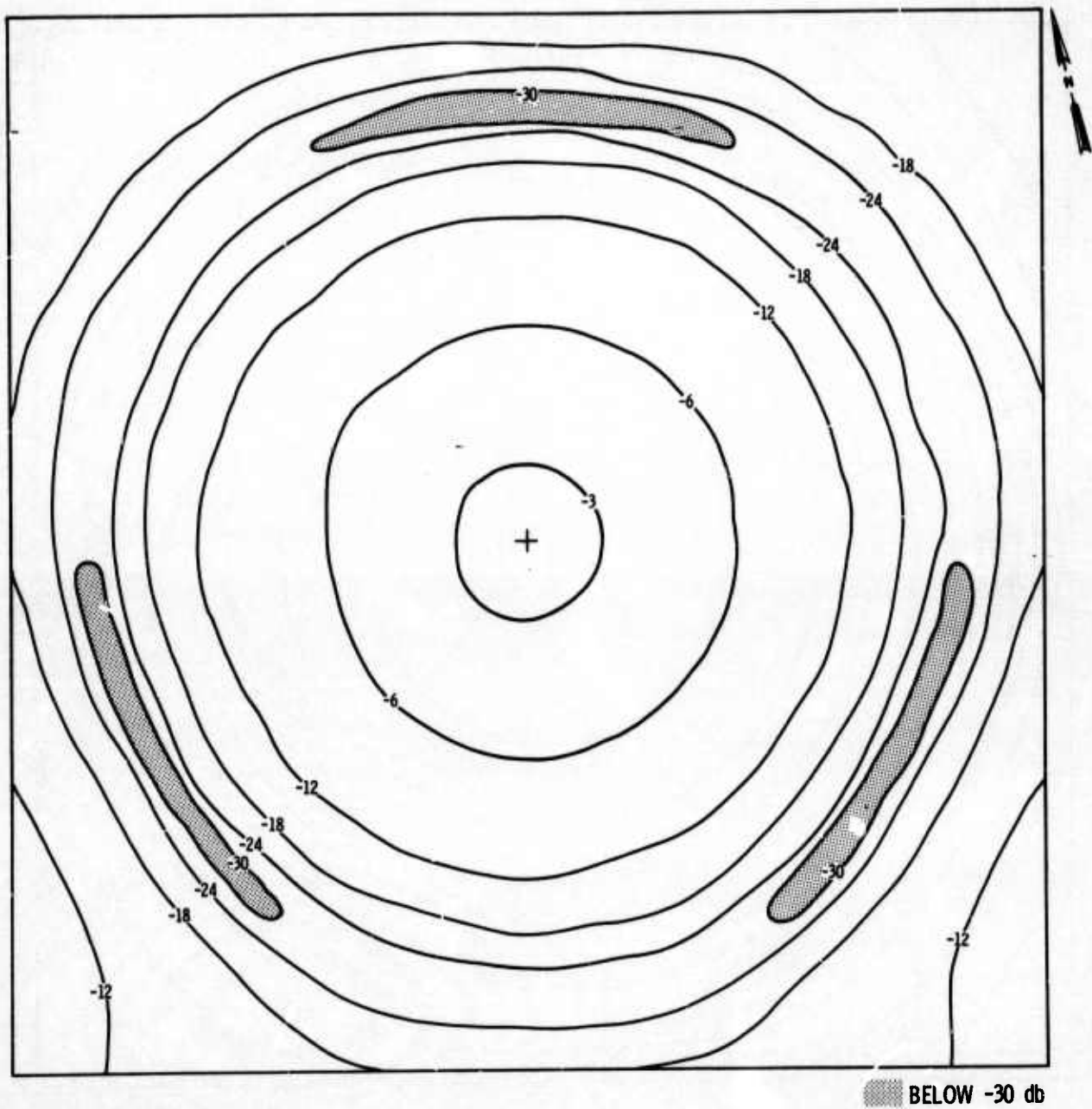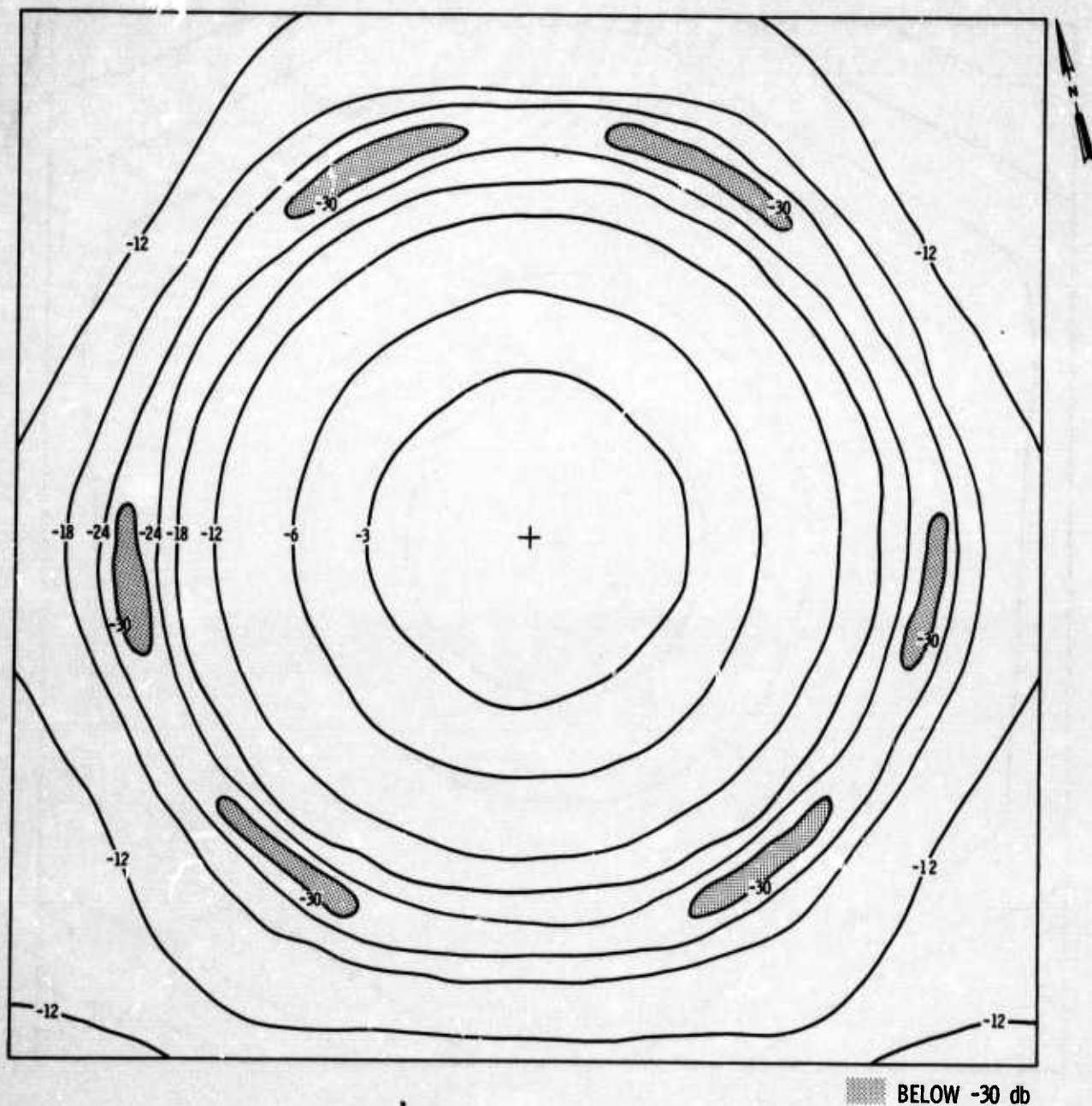Figure 27. MCF A1 f-$\vec{k}$ Response at 0.50 Hz

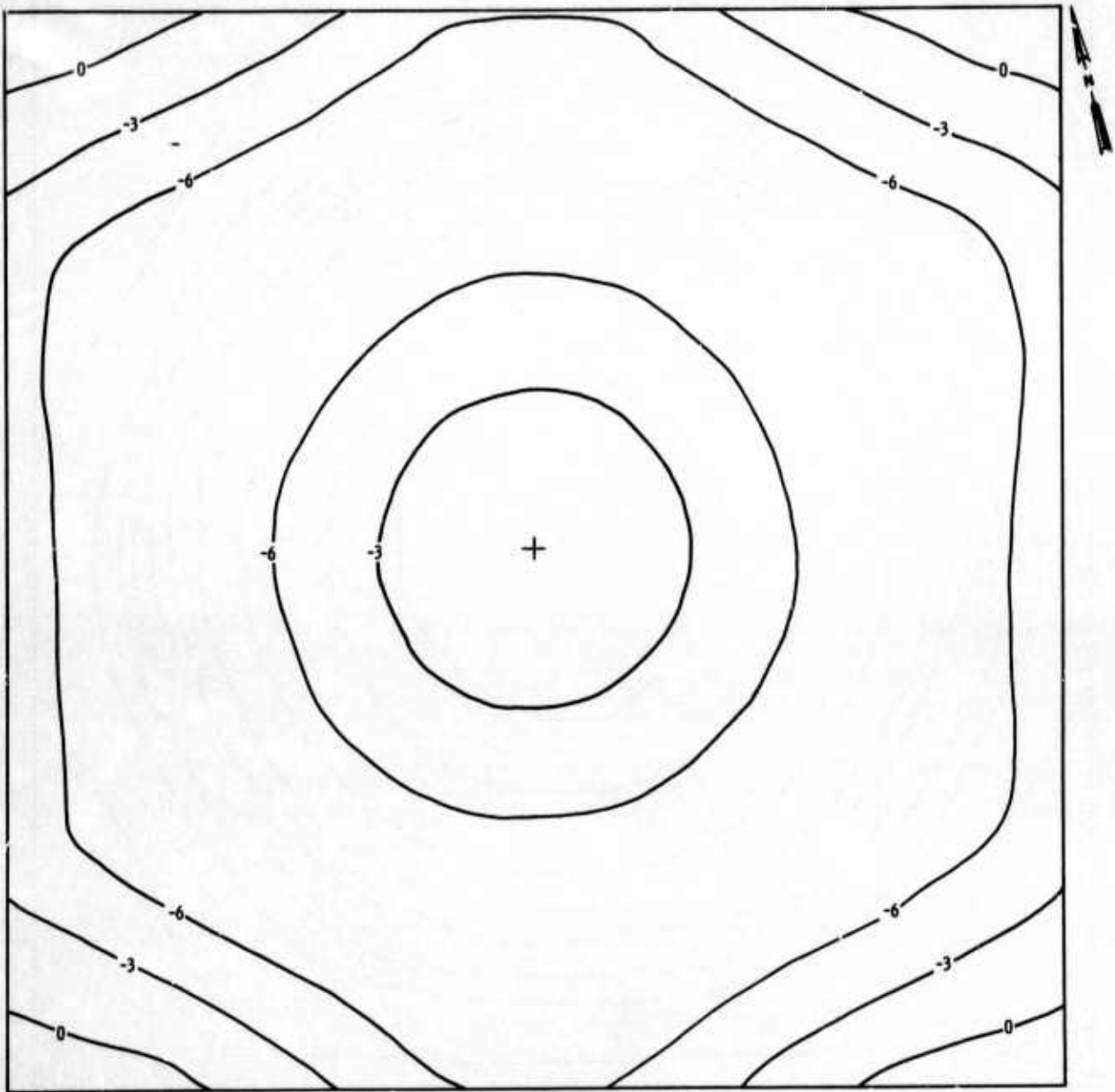Figure 28. IP 9 f-$\vec{k}$ Response at 0.50 Hz

Figure 29. MCF A1 f-$\vec{k}$ Response at 0.75 Hz

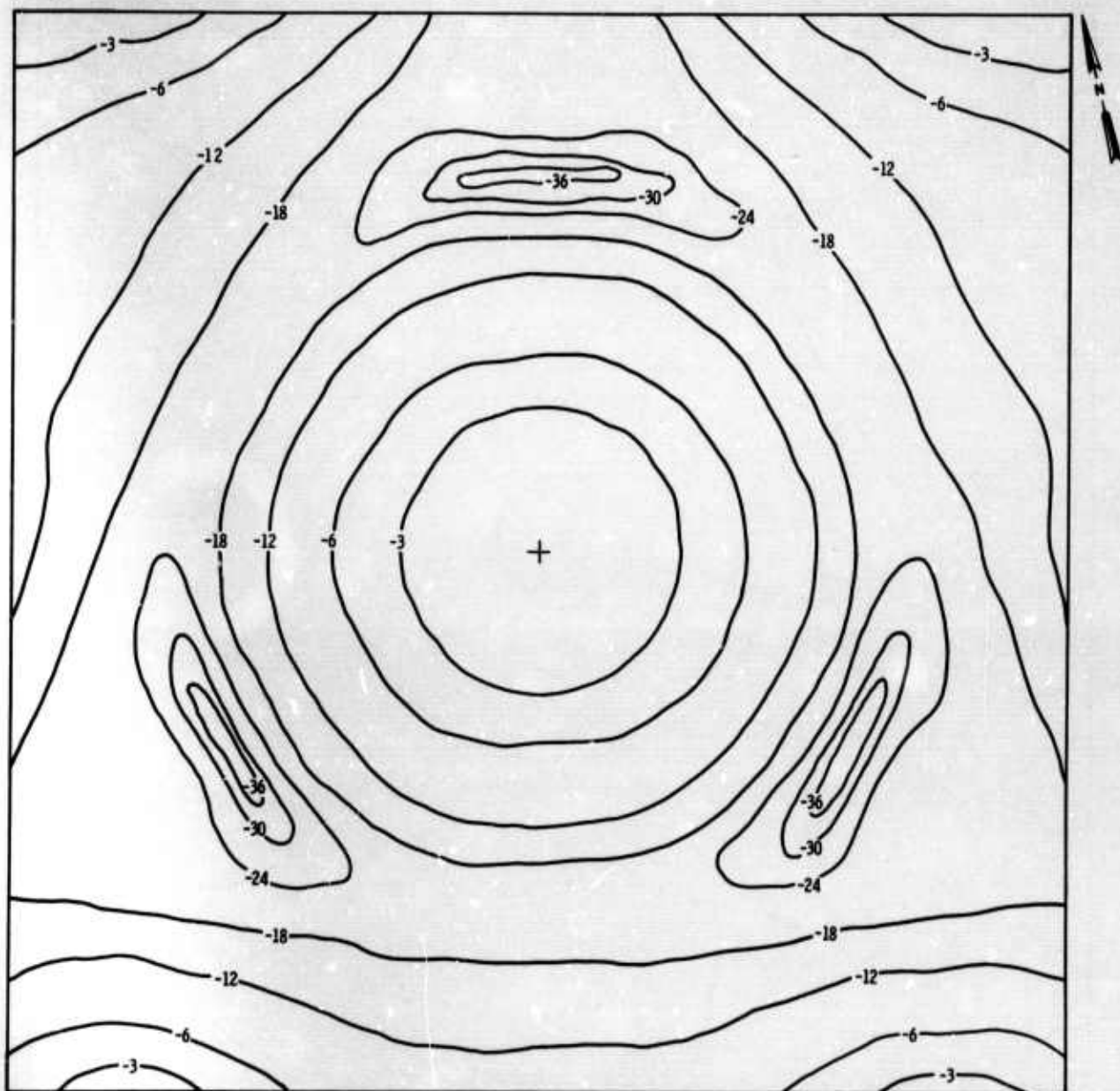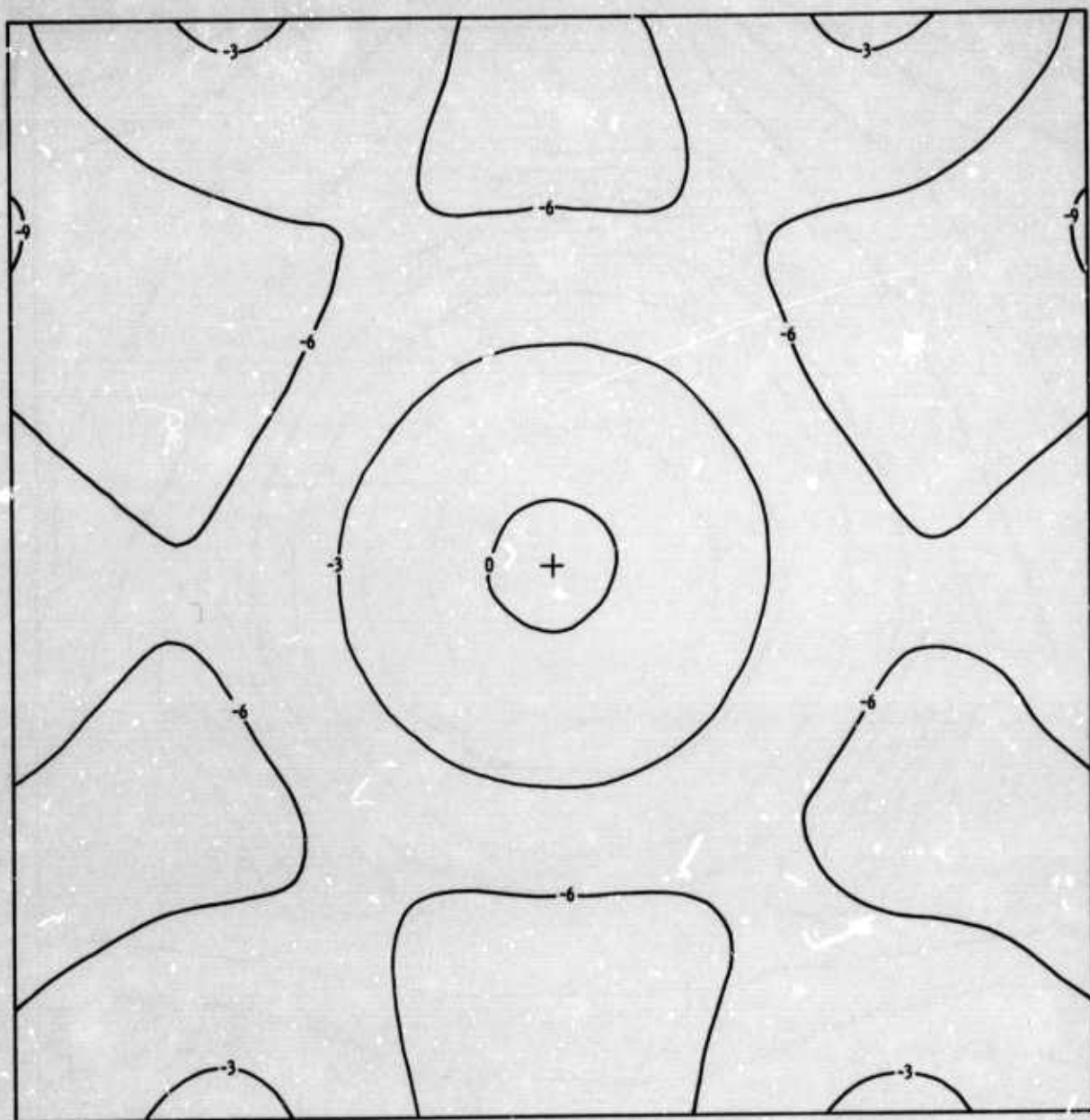Figure 30. IP 9 f-$\vec{k}$ Response at 0.75 Hz

Figure 31.   MCF A1 f-$\vec{k}$ Response at 1.0 Hz
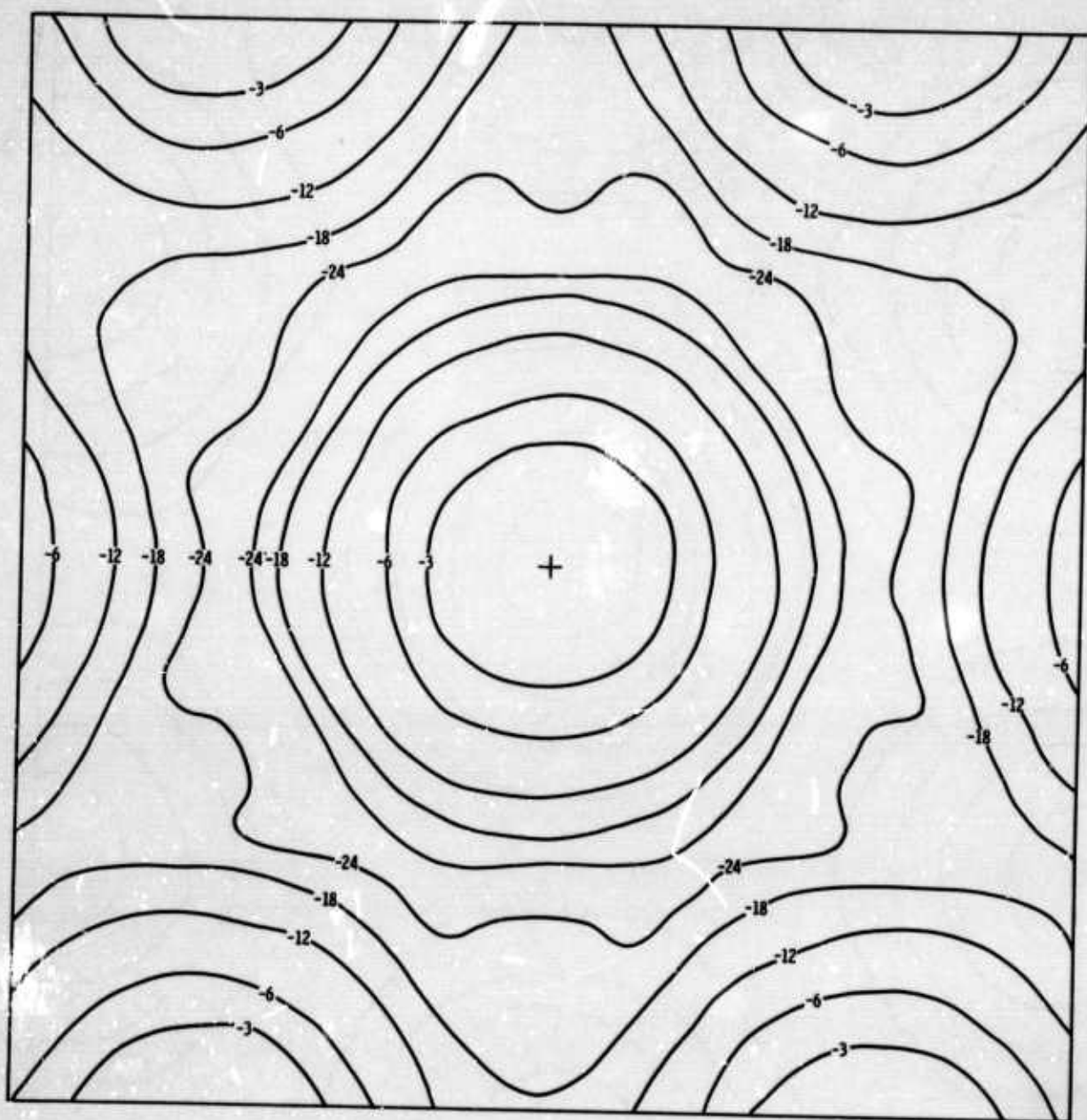
Figure 32.   IP 9 f-$\vec{k}$ Response at 1.0 Hz
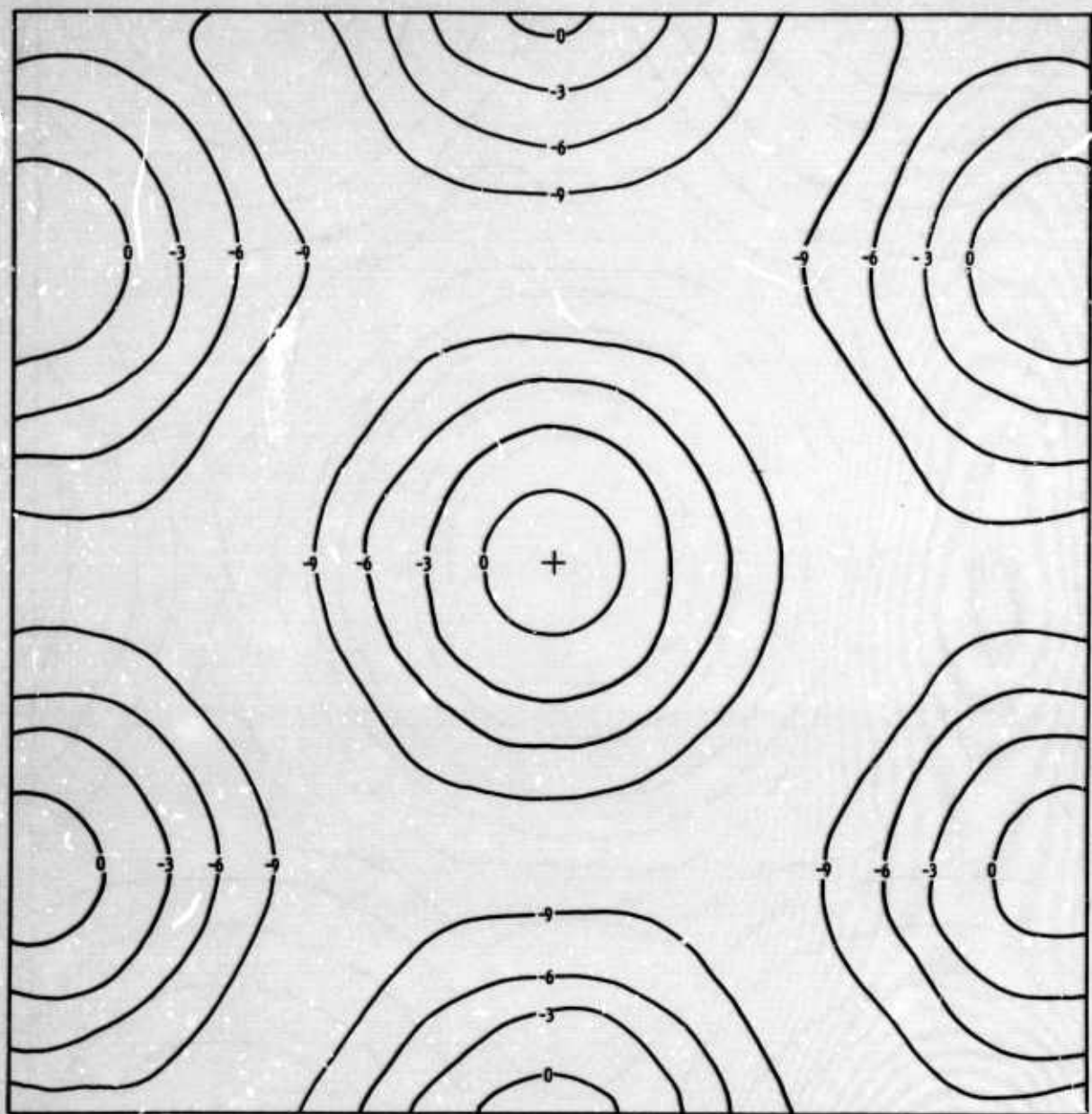
Figure 33. MCF A1 f-$\vec{k}$ Response at 2.0 Hz
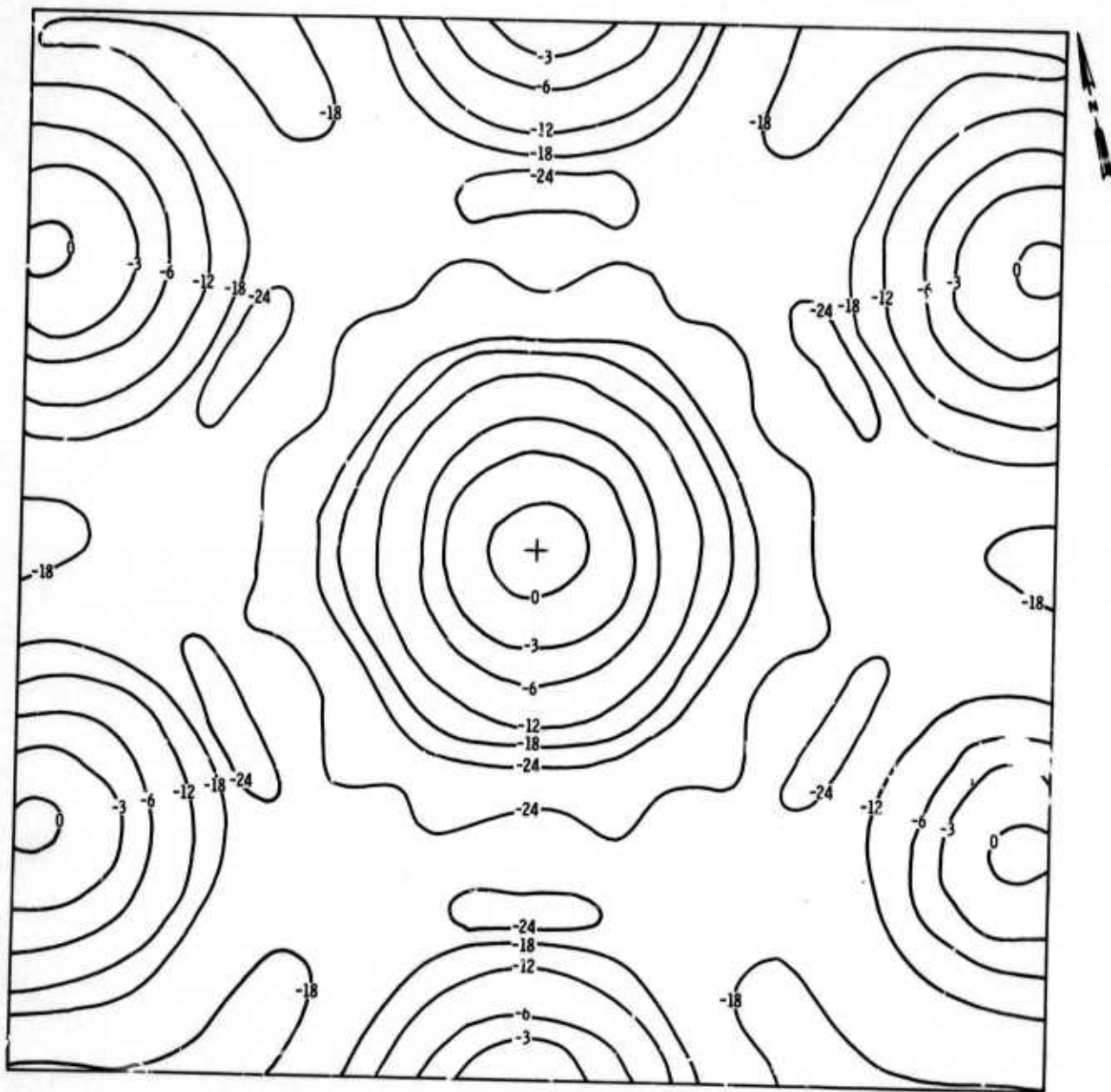
Figure 34. IP 9 f-$\vec{k}$ Response at 2.0 Hz

SECTION IV

USE OF ARRAY GEOMETRIES IN THE
DESIGN OF MULTICHANNEL FILTERS

One purpose of this study was to investigate the use of various array geometries for the design of multichannel filters. Table 1 lists the filters which were designed using local noise.

Table 1

DESIGN OF LOCAL NOISE FILTERS

Filter	Array Geometry	S/N Ratio	Event
MCF A1	A	1.0	Crete
MCF A2	A	0.1	Crete
MCF A3	A	1.0	Peru
MCF A4	A	1.0	BB
MCF A5	A	1.0	CC
MCF B1	B	1.0	Crete
MCF B2	B	1.0	Peru
MCF B3	B	1.0	BB
MCF B5	B	1.0	CC
MCF C1	C	1.0	Crete
MCF C2	C	1.0	Peru
MCF C3	C	1.0	BB
MCF C4	C	1.0	CC

Figures 35 through 46 present the results of the array geometry study. Figure 35 is the result of applying MCF A1, the 5-ring filter, to the Crete event; Figure 36 is the result of applying MCF B1, a 6-channel (4-triplet, 2-ring) filter to the same event. There is very little difference between these two outputs. Figure 37 is the output of MCF C1, a 6-channel (4-triplet, 2-ring) filter applied to the Crete event; its output does not differ significantly from the outputs of MCF A1 and MCF B1.

Figure 38 is the output of MCF A3, a 5-ring filter designed using the Peru event which had the unusually high S/N ratio of 17:1. While the filter does a good job, the straight sum does almost as well because of the large S/N ratio. Figures 39 and 40 indicate that little difference occurs when changing the array geometry from five channels to six for the Peru event.

Figure 41 is the output of MCF A4, which was designed from and applied to Quarry Blast BB. The signal model was the segment of time trace Z 10 from just before the arrival of the P-wave to the end of the record. The MCF provides about 6-db S/N improvement over the low-frequency noise. Figures 42 and 43 indicate that little is gained in developing a 6-channel filter for Quarry Blast BB (compared to the 5-channel filter).

Figure 44 is the output of MCF A5, a 5-ring filter designed from and applied to Quarry Blast CC. The results are essentially the same as for Quarry Blast BB, i.e., approximately 6-db improvement over the low-frequency noise. Figure 45 shows that there is a slight improvement when using six channels rather than five channels for Quarry Blast CC. Figure 46 shows that MCF C4 is slightly better than MCF A3 and MCF B4 in rejecting noise; however, the difference is almost insignificant. Probably, a better way to design a filter to pass these quarry blasts would be to include in the signal model only the first few seconds of P-motion and S-motion through the major portion of the L-R motion while skipping the noise between the P- and S-motion; then, the filter would be better able to reject the noise.

In conclusion, the study of array geometries in the design of multichannel filters has shown that changing the array geometry does not seriously affect the output of the filters.
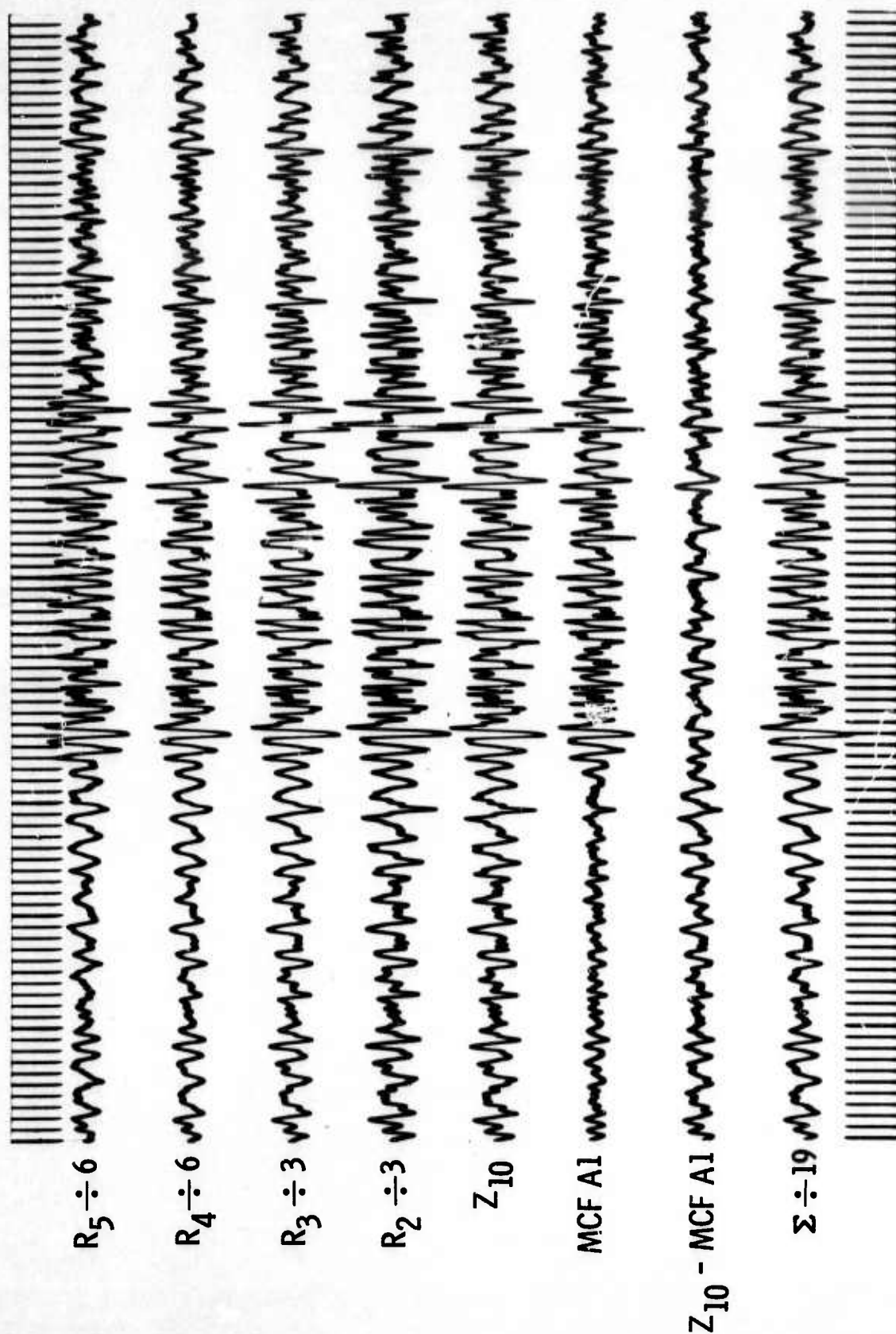
Figure 35. Outputs for MCF A1, Crete Event, Teleseism AA

$R_5 \div 6$

$R_4 \div 6$

$R_3 \div 3$

$R_2 \div 3$

Z_{10}

MCF A1

Z_{10} - MCF A1

$\Sigma \div 19$
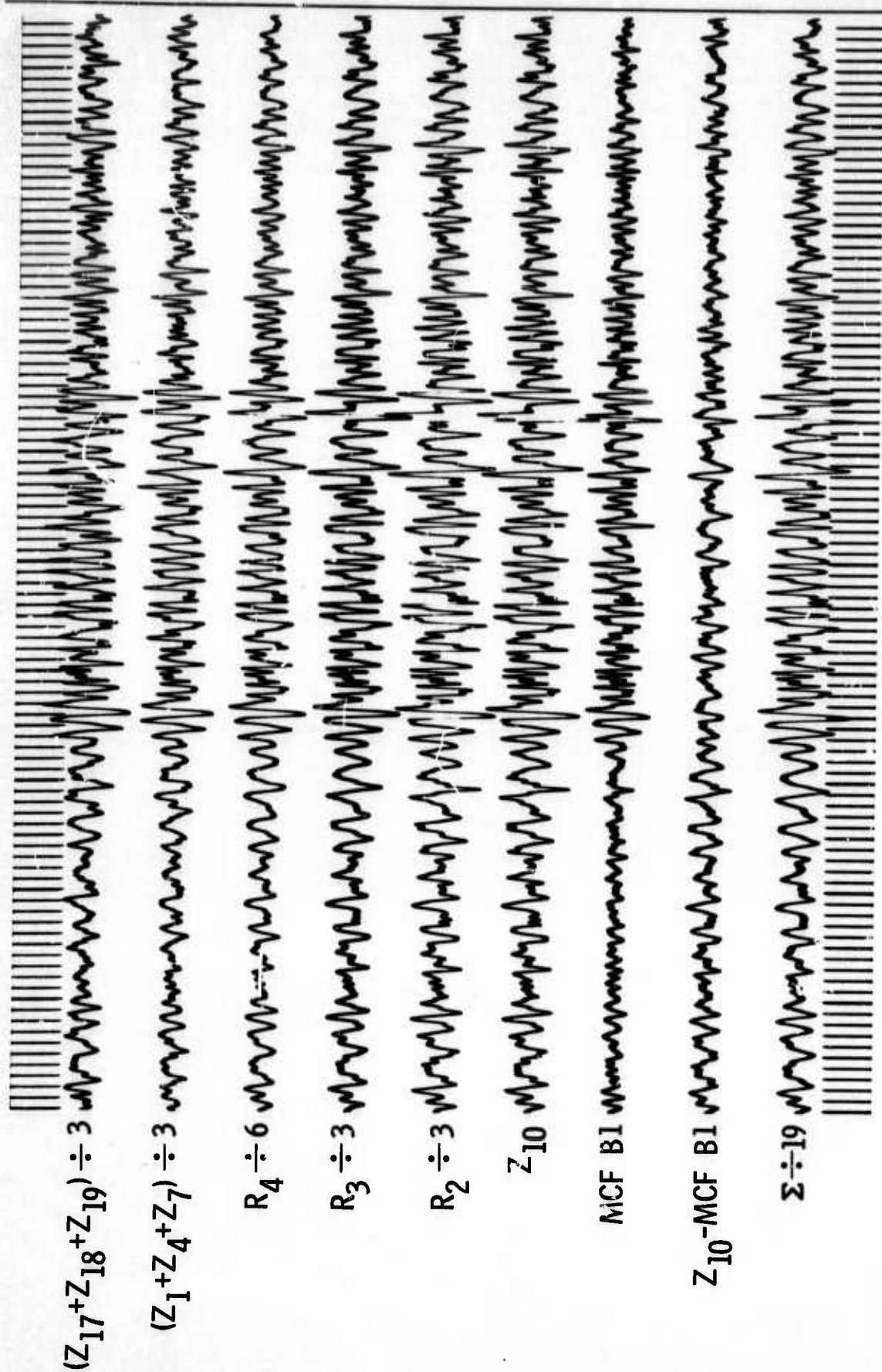
Figure 36. Outputs for MCF B1, Crete Event, Teleseism AA

$(Z_{17} + Z_{18} + Z_{19}) \div 3$

$(Z_1 + Z_4 + Z_7) \div 3$

$R_4 \div 6$

$R_3 \div 3$

$R_2 \div 3$

Z_{10}

MCF B1

Z_{10}-MCF B1

$\Sigma \div 19$
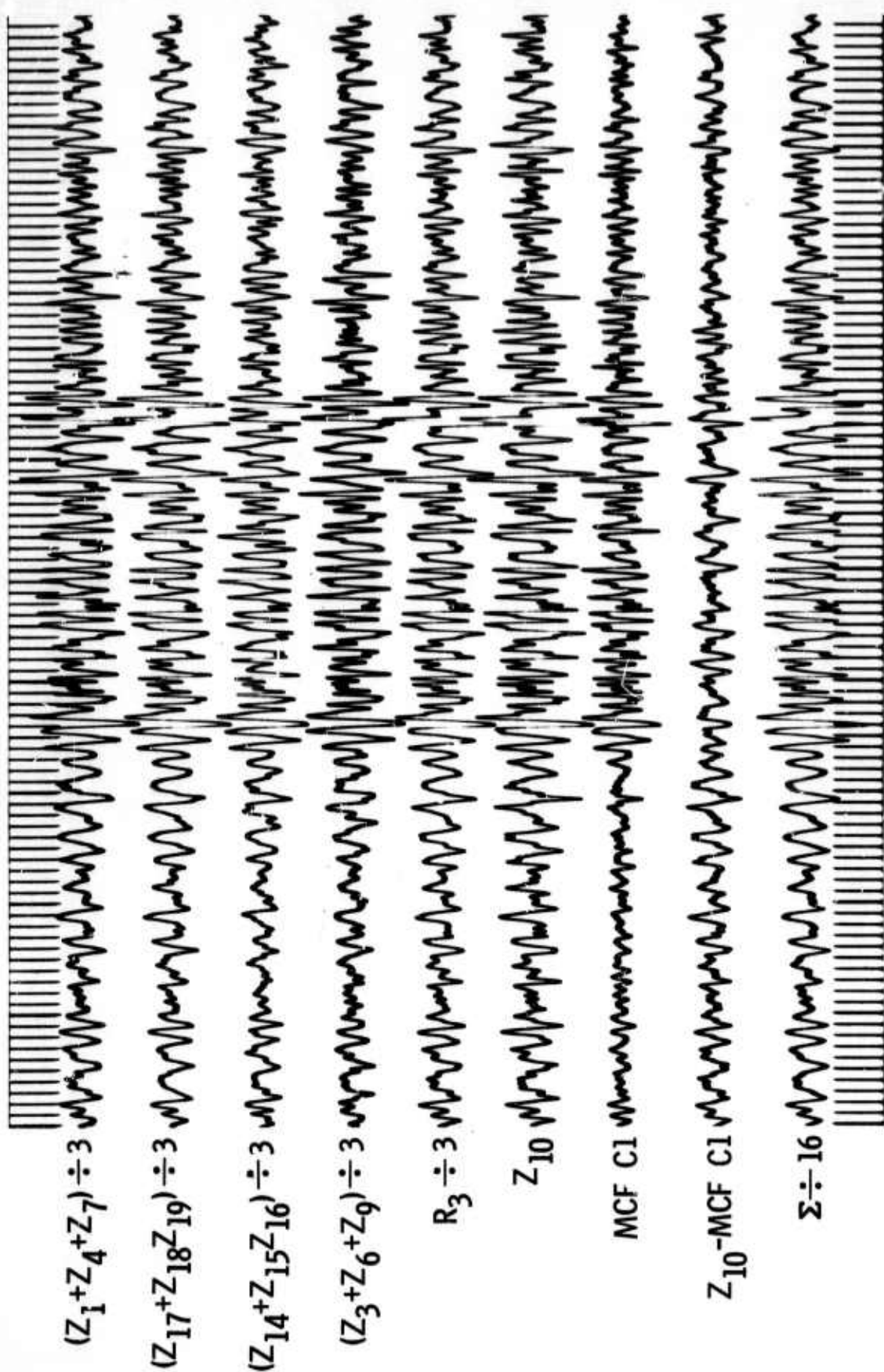
Figure 37. Outputs for MCF C1, Crete Event, Teleseism AA

$(Z_1 + Z_4 + Z_7) \div 3$

$(Z_{17} + Z_{18} Z_{19}) \div 3$

$(Z_{14} + Z_{15} Z_{16}) \div 3$

$(Z_3 + Z_6 + Z_9) \div 3$

$R_3 \div 3$

Z_{10}

MCF C1

Z_{10}-MCF C1

$\Sigma \div 16$
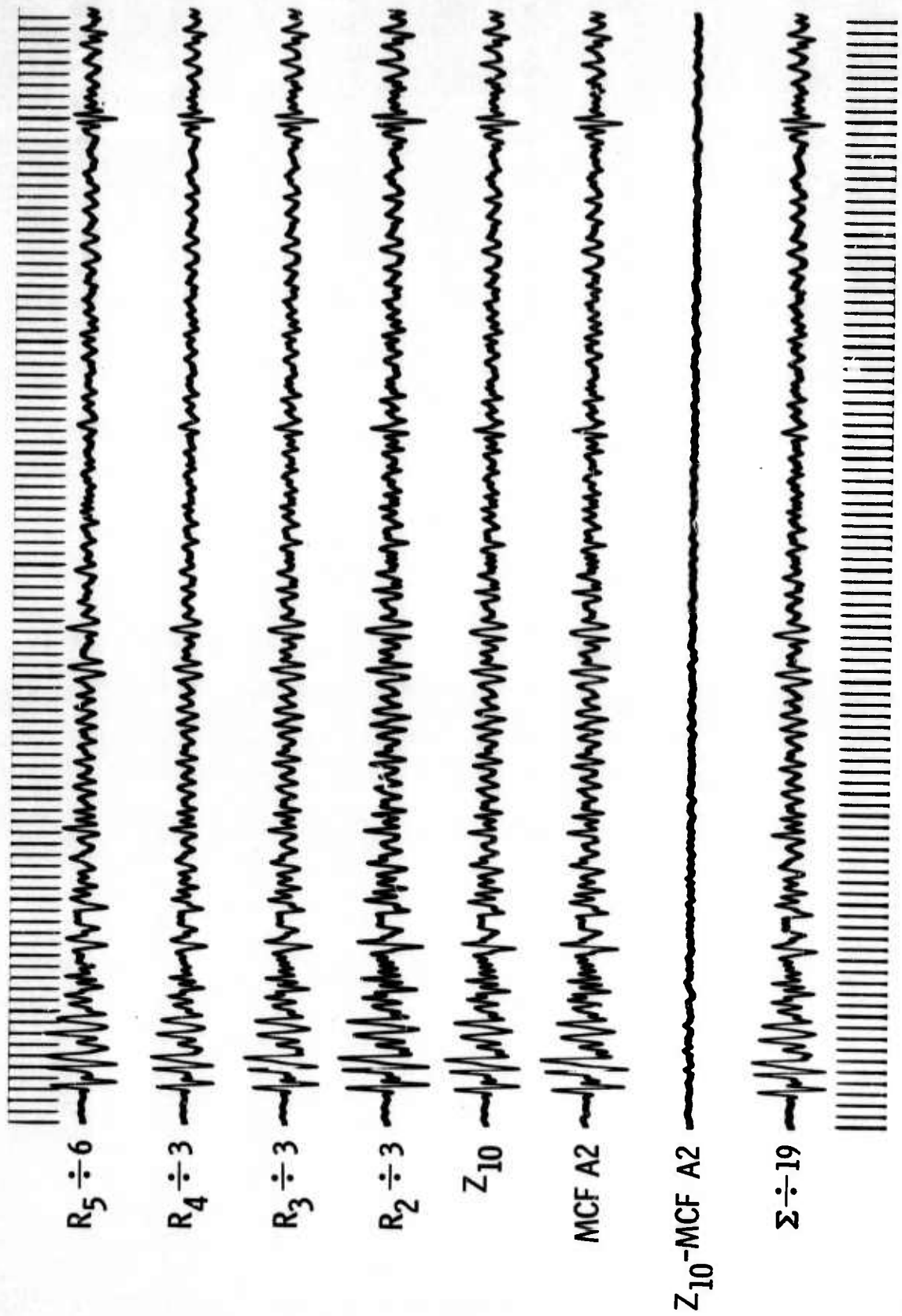
Figure 38. Outputs for MCF A3, Peru Event, Teleseism BB

R₅ ÷ 6

R₄ ÷ 3

R₃ ÷ 3

R₂ ÷ 3

Z₁₀

MCF A2

Z₁₀-MCF A2

Σ ÷ 19

$(Z_{17}+Z_{18}+Z_{19}) \div 3$

$Z_1+Z_4+Z_7) \div 3$

$R_4 \div 6$

$R_3 \div 3$

$R_2 \div 3$

Z_{10}

MCF B2

$Z_{10}-$MCF B2

$\Sigma \div 19$
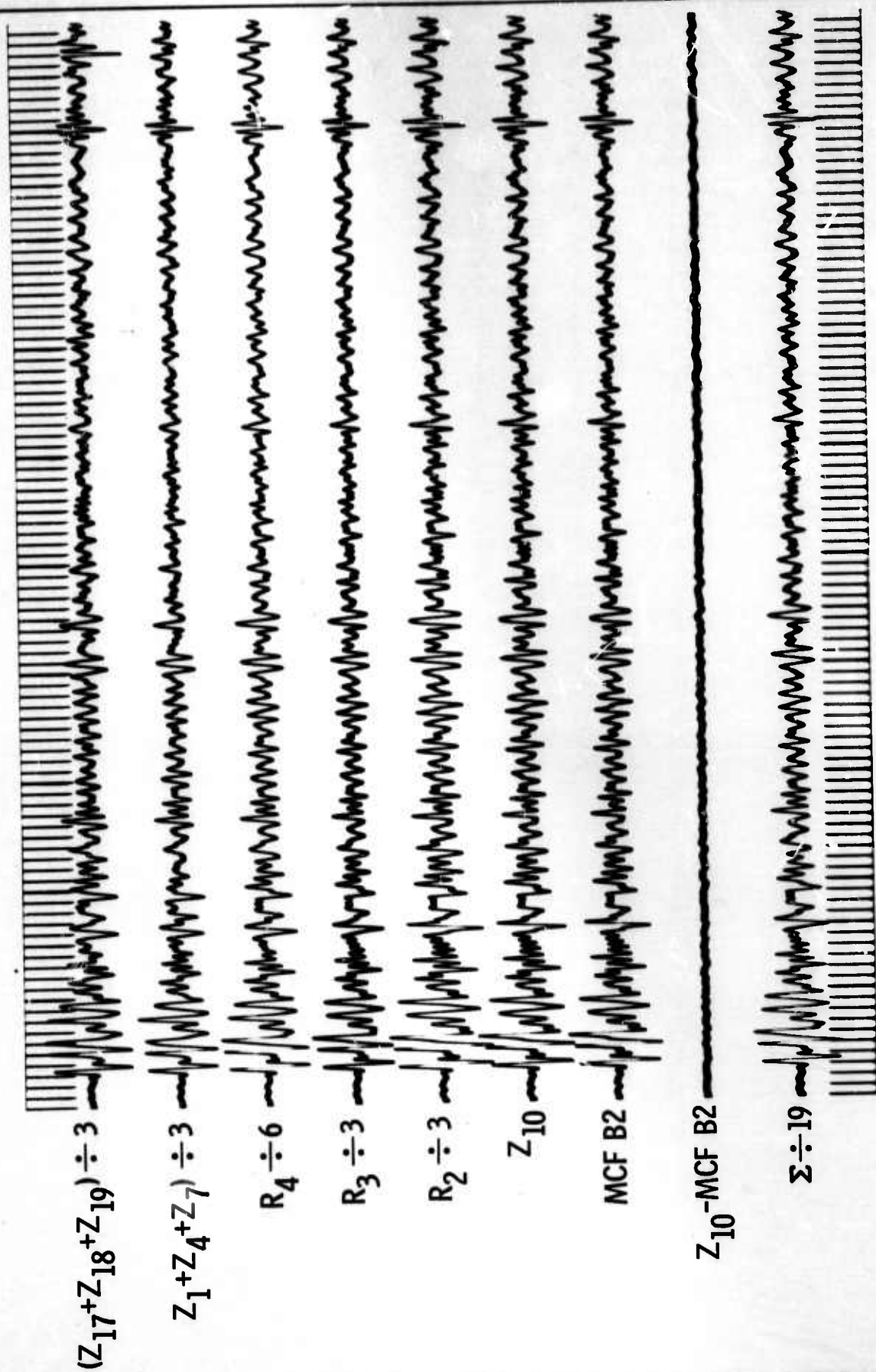
Figure 39.   Outputs for MCF B2, Peru Event, Teleseism BB
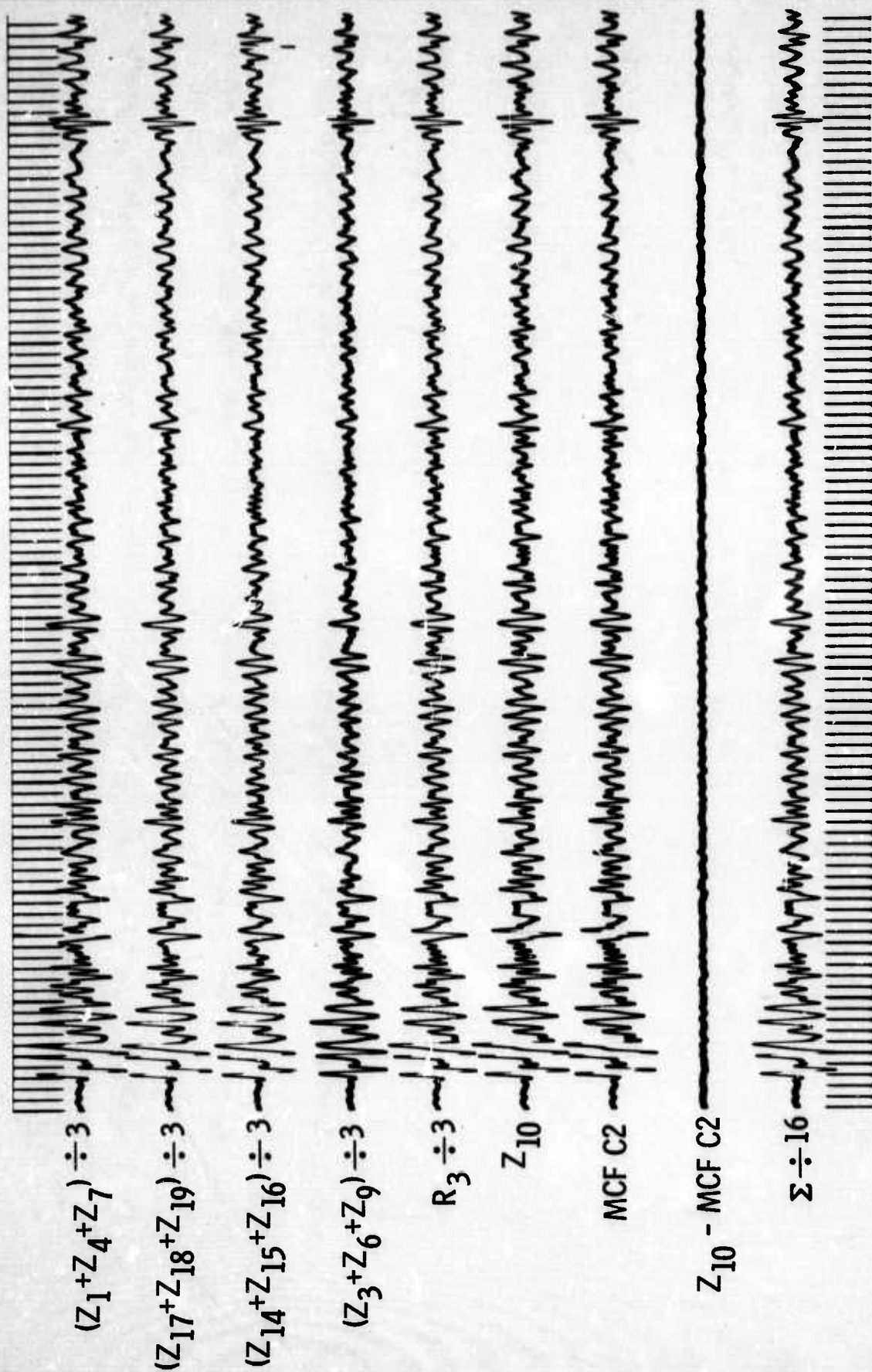
Figure 40. Outputs for MCF C2, Peru Event, Teleseism BB

The traces are labeled:
$(Z_1 + Z_4 + Z_7) \div 3$
$(Z_{17} + Z_{18} + Z_{19}) \div 3$
$(Z_{14} + Z_{15} + Z_{16}) \div 3$
$(Z_3 + Z_6 + Z_9) \div 3$
$R_3 \div 3$
Z_{10}
MCF C2
$Z_{10} - $ MCF C2
$\Sigma \div 16$
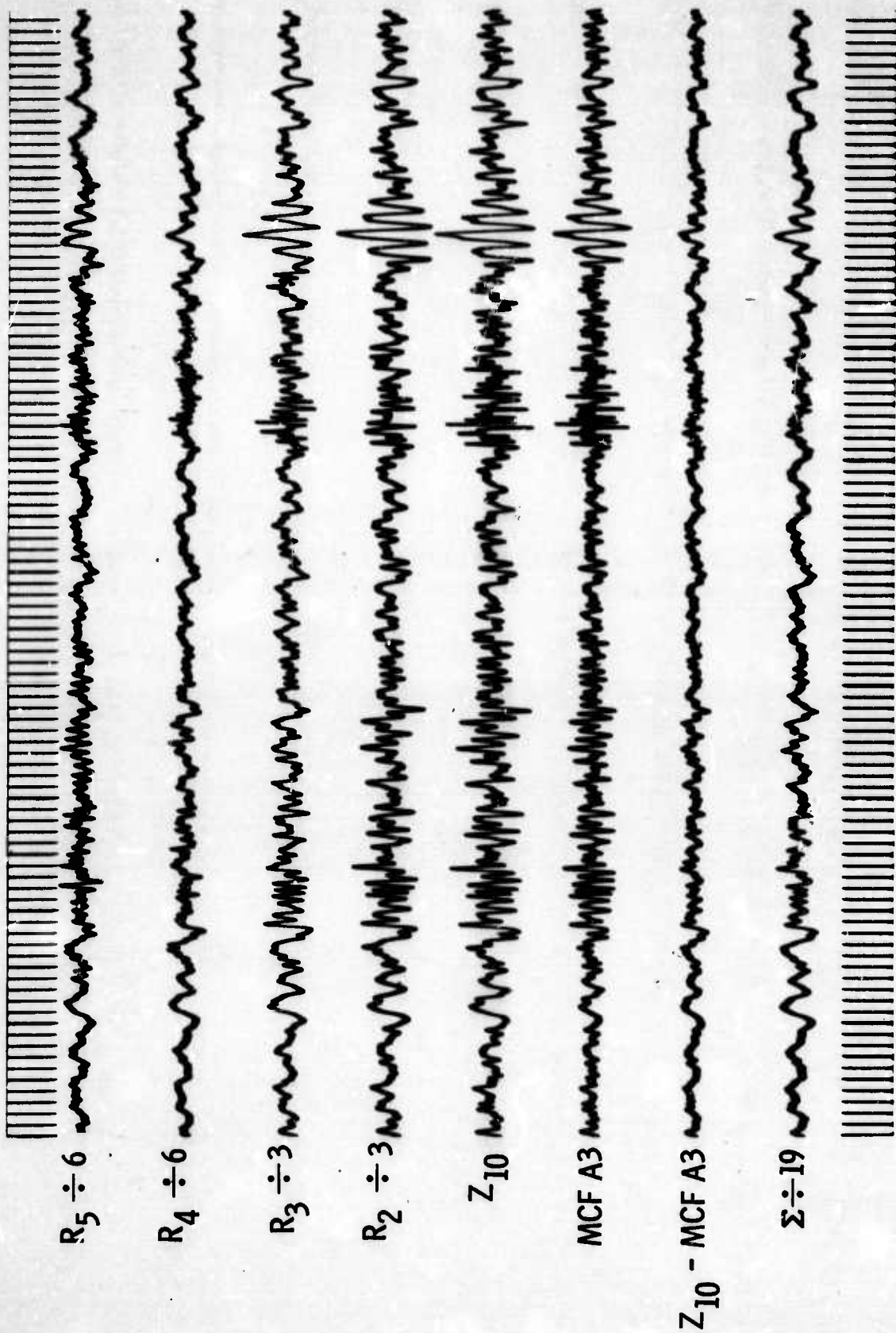
Figure 41. Outputs for MCF A4, Quarry Blast BB

R₅ ÷ 6

R₄ ÷ 6

R₃ ÷ 3

R₂ ÷ 3

Z₁₀

MCF A3

Z₁₀ - MCF A3

Σ ÷ 19

$(Z_{17}+Z_{18}+Z_{19}) \div 3$

$(Z_1+Z_4+Z_7) \div 3$

$R_4 \div 6$

$R_3 \div 3$

$R_2 \div 3$

Z_{10}

MCF B3

Z_{10} - MCF B3

$\Sigma \div 19$
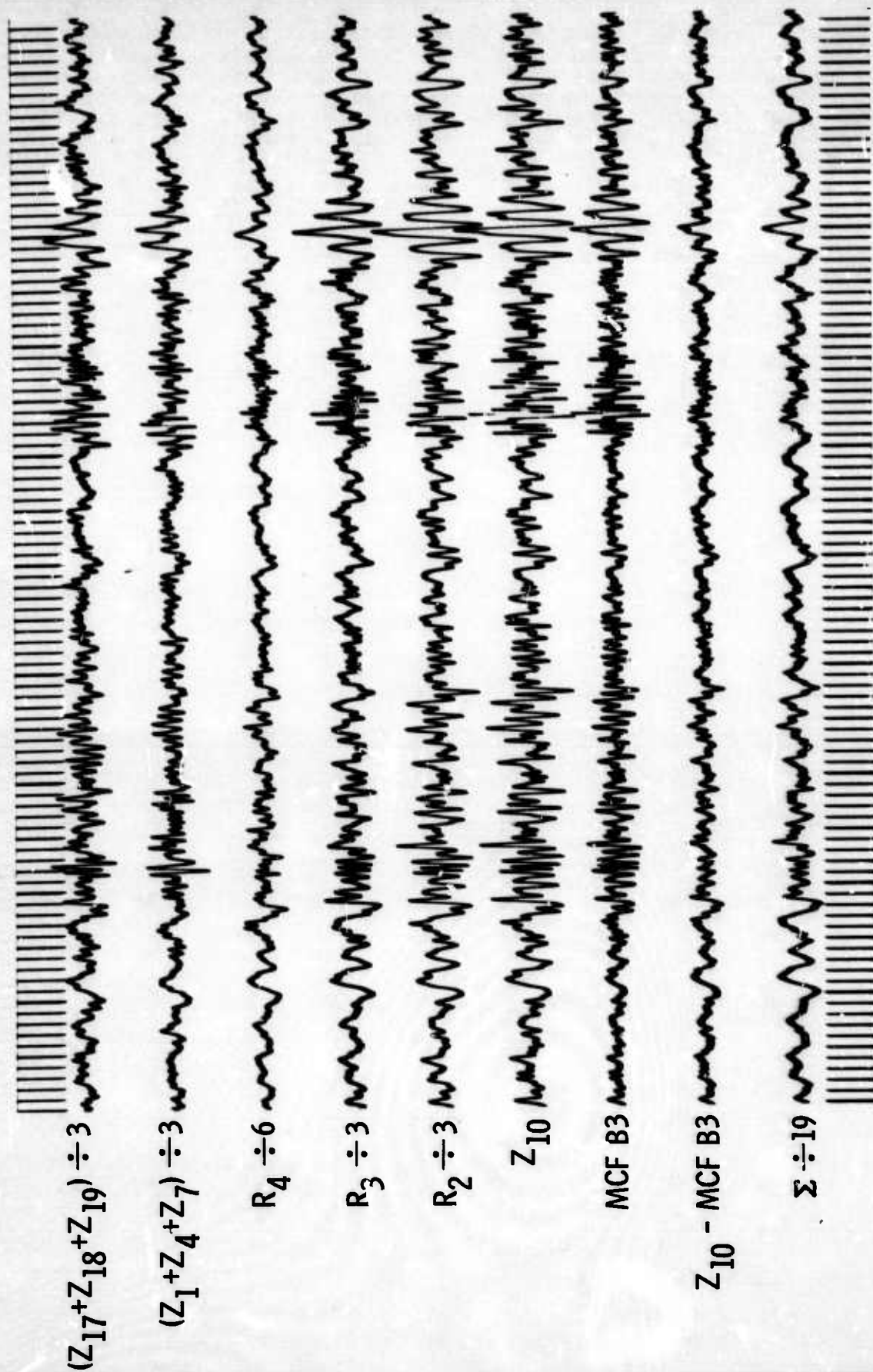
Figure 42. Outputs for MCF B3, Quarry Blast BB
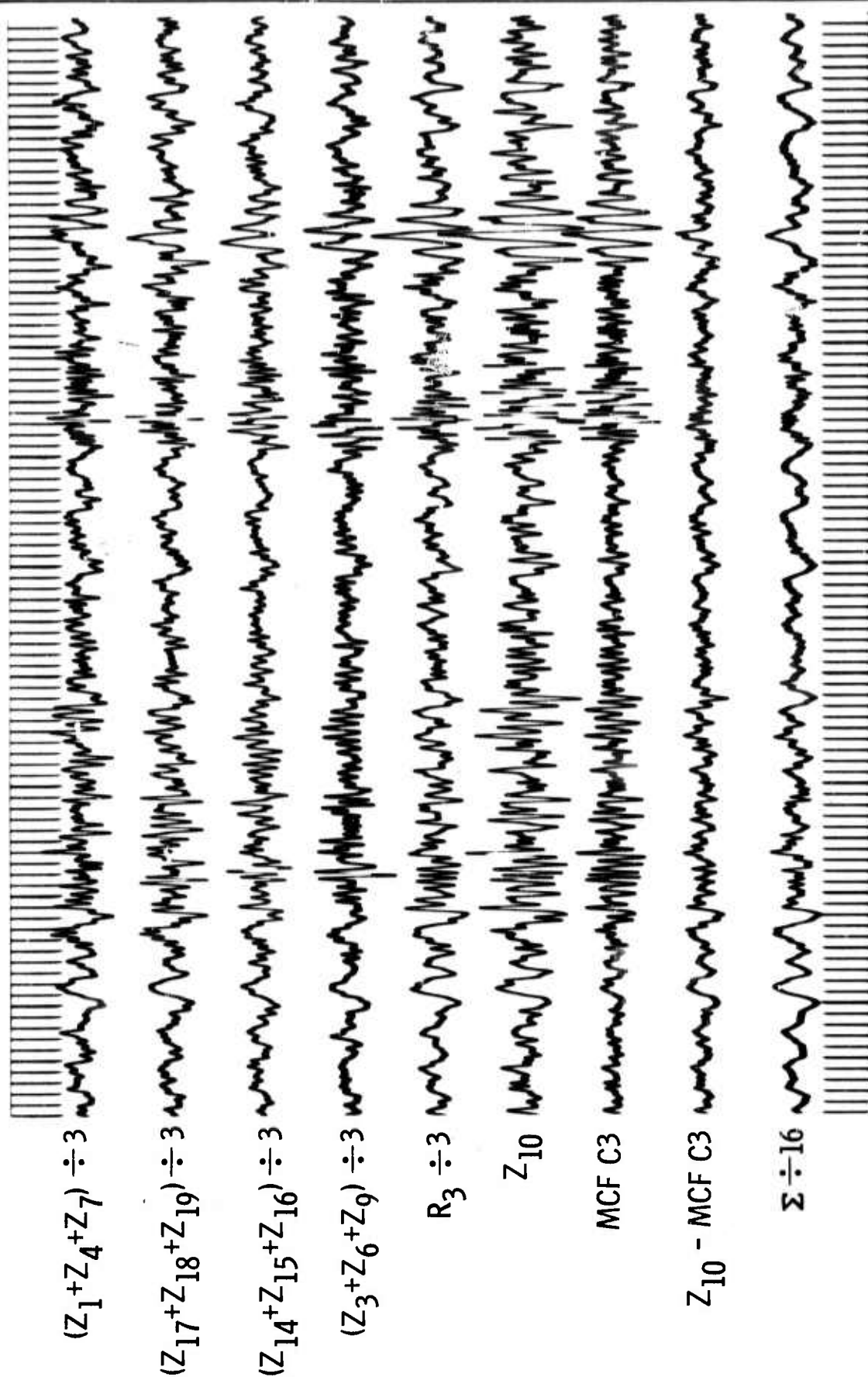
Figure 43. Outputs for MCF C3, Quarry Blast BB

$(Z_1 + Z_4 + Z_7) \div 3$

$(Z_{17} + Z_{18} + Z_{19}) \div 3$

$(Z_{14} + Z_{15} + Z_{16}) \div 3$

$(Z_3 + Z_6 + Z_9) \div 3$

$R_3 \div 3$

Z_{10}

MCF C3

Z_{10} - MCF C3

$\Sigma \div 16$

science services division

R$_5$ $\div$ 6

R$_4$ $\div$ 6

R$_3$ $\div$ 3

R$_2$ $\div$ 3

Z$_{10}$

MCF A4

Z$_{10}$ - MCF A4

$\Sigma \div$ 19
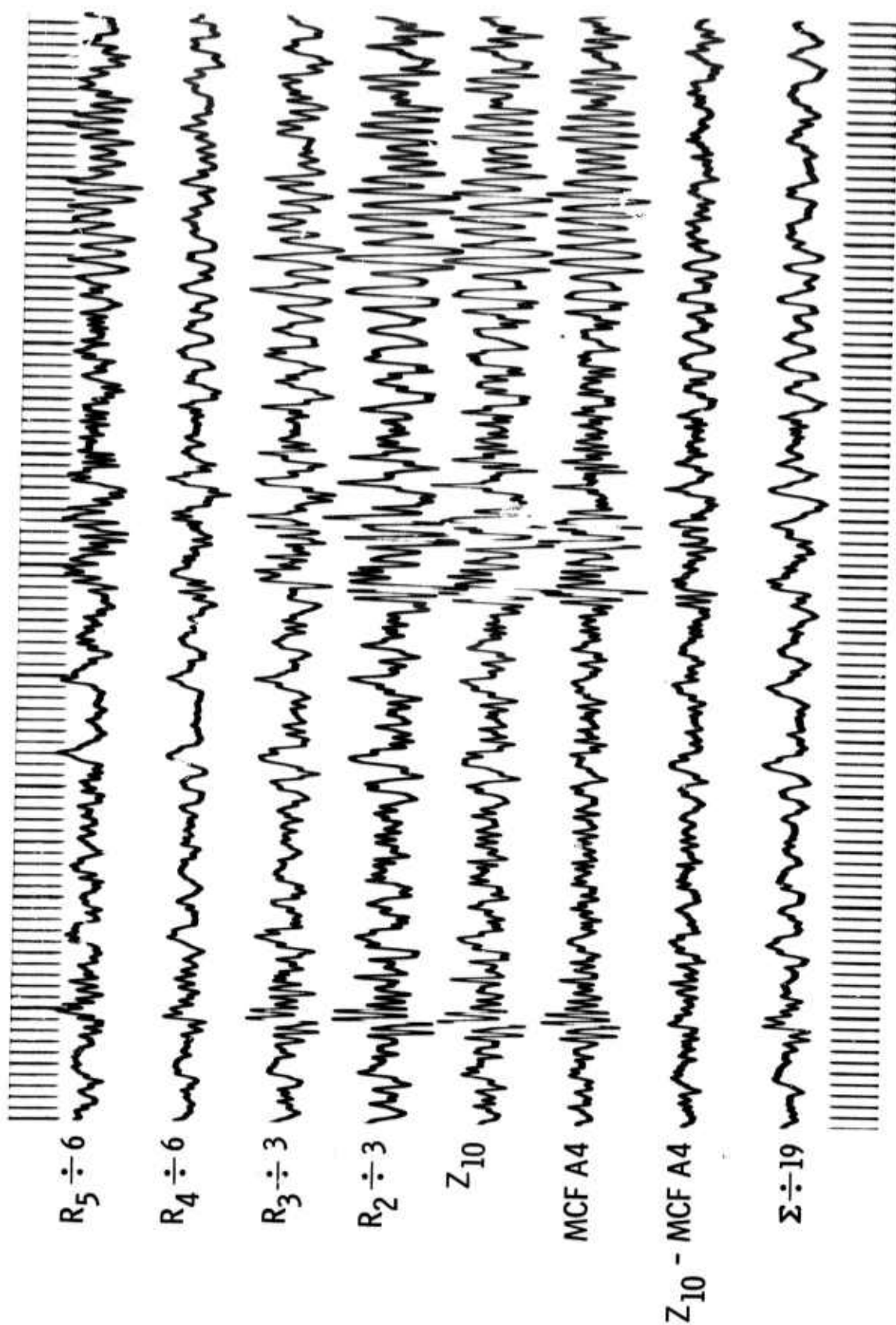
Figure 44. Outputs for MCF A5, Quarry Blast CC

55
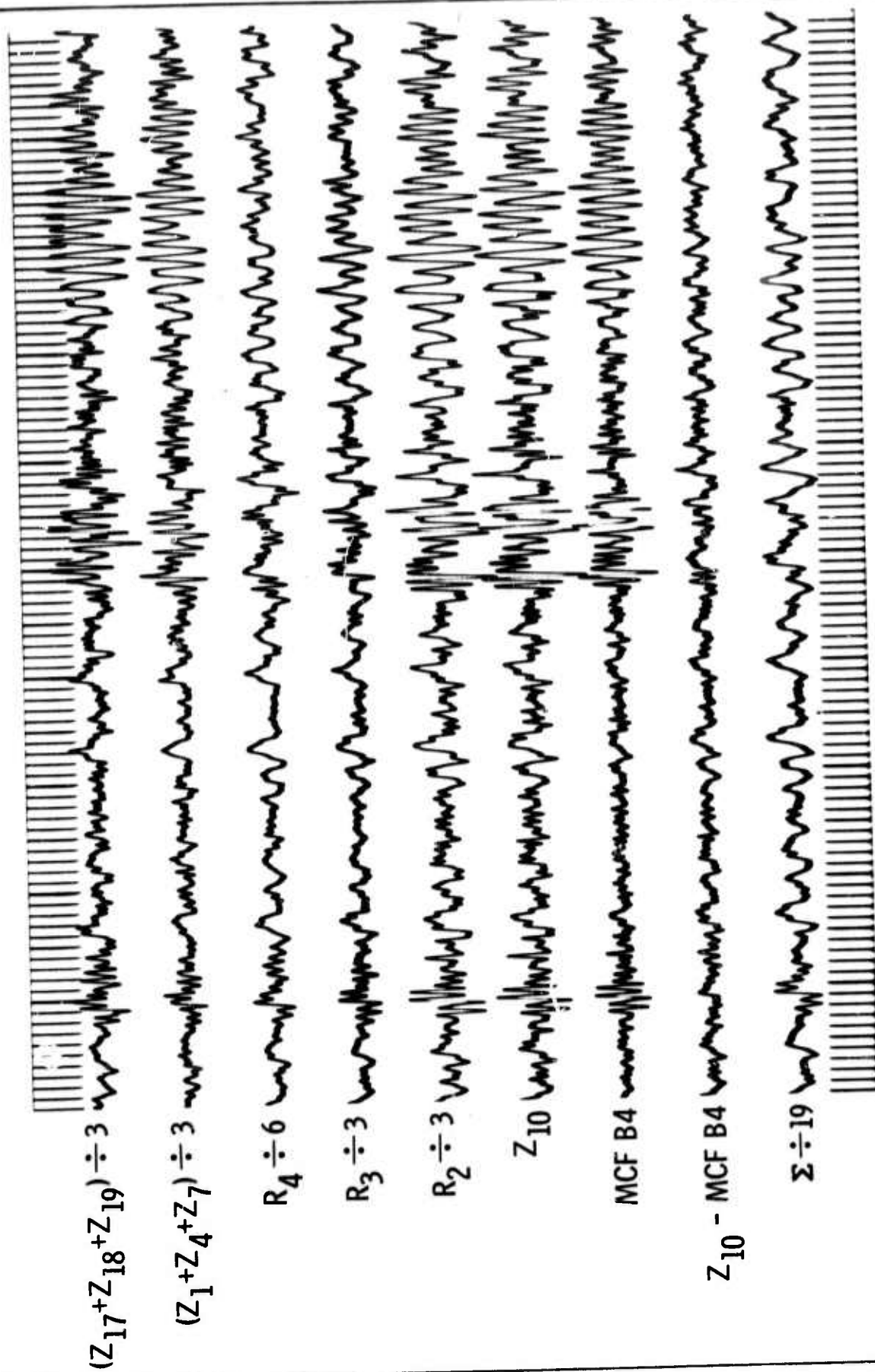
Figure 45. Outputs for MCF B4, Quarry Blast CC

$(Z_{17}+Z_{18}+Z_{19}) \div 3$

$(Z_1+Z_4+Z_7) \div 3$

$R_4 \div 6$

$R_3 \div 3$

$R_2 \div 3$

Z_{10}

MCF B4

Z_{10} - MCF B4

$\Sigma \div 19$

$(Z_1+Z_4+Z_7) \div 3$

$(Z_{17}+Z_{18}+Z_{19}) \div 3$

$(Z_{14}+Z_{15}+Z_{16}) \div 3$

$(Z_3+Z_6+Z_9) \div 3$

$R_3 \div 3$

Z_{10}

MCF C4

Z_{10} - MCF C4

$\Sigma \div 16$
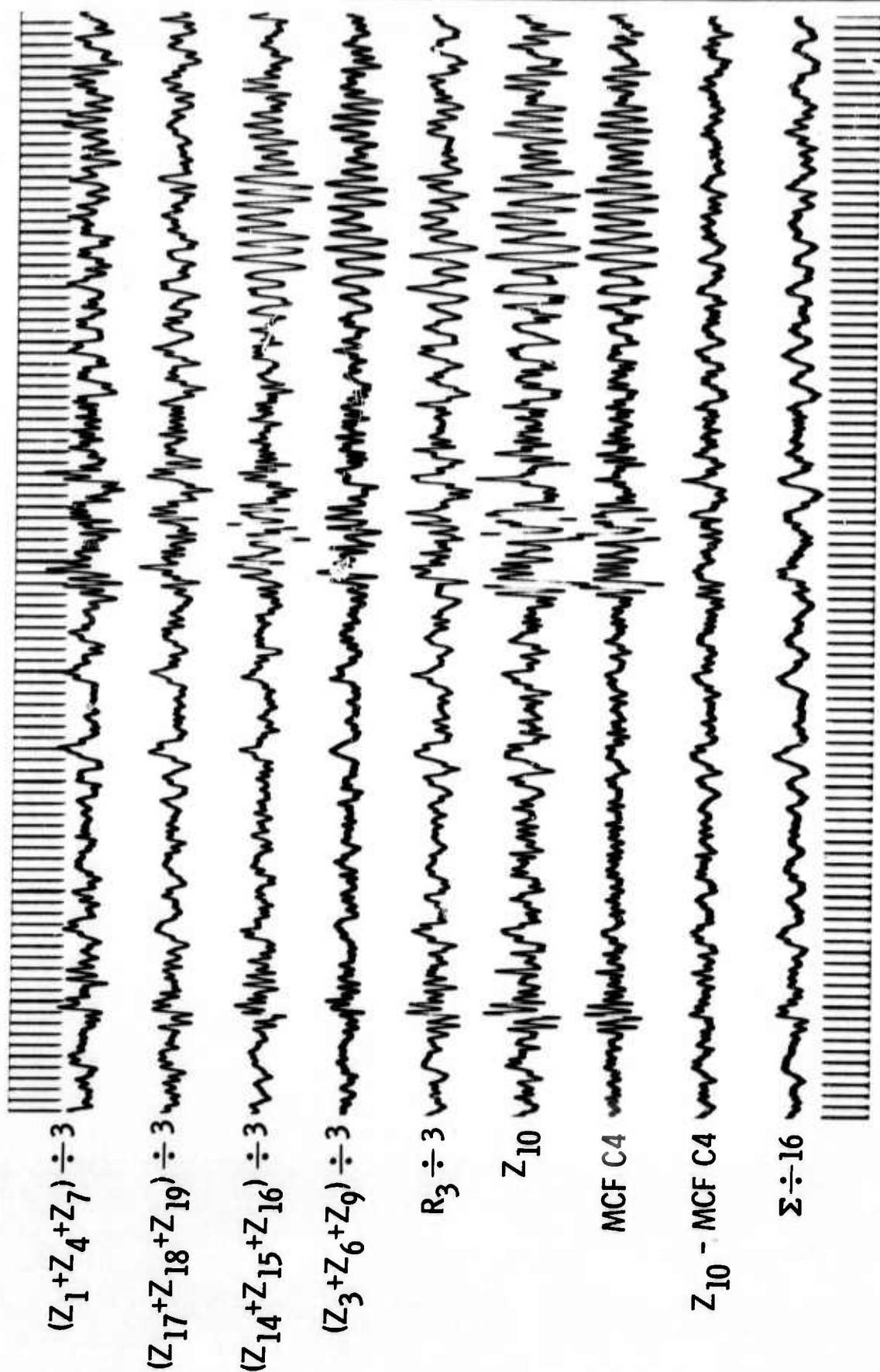
Figure 46. Outputs for MCF C4, Quarry Blast CC

science services division

SECTION V

CONCLUSIONS

From this study, it can be concluded that:

- An effective method of overcoming gain inequalities while preserving signal and rejecting a reasonable amount of noise is to use local noise and signals to design signal-extraction multichannel filters.

- Study of the output of local noise filter MCF A1 and IP 9 indicates that IP 9 exhibits excessive gain attenuation for teleseismic signals, which can be attributed to either gain inequalities in the noise model or an insufficient amount of gain variation added to the signal model.

- Variations in S/N ratios give no significant gain in S/N improvement.

- Designing multichannel filters on various array geometries has little effect on their final output.